

**Humanization of Yeast Exosome Protein Selection Machinery to Investigate Functional
Evolutionary Conservation**

Curtis John Logan

A Thesis In The Department of Biology

Presented in Partial Fulfillment of the Requirements
For the Degree of Master of Science (Biology)
at Concordia University
Montréal, Québec, Canada

January 2023

© Curtis John Logan, 2023

Concordia University
School of Graduate Studies

This is to certify that the thesis prepared

By: Curtis John Logan

Entitled: **Humanization of Yeast Exosome Protein Selection Machinery to Investigate
Functional Evolutionary Conservation**

and submitted in partial fulfillment of the requirements for the degree of

Master of Science (Biology)

complies with the regulations of the University and meets the accepted standards with respect to originality and quality.

Signed by the final Examining Committee:

_____ Chair
Dr. Vincent Martin

_____ External Examiner
Dr. David Kwan

_____ Examiner
Dr. Malcolm Whiteway

_____ Thesis Supervisor
Dr. Christopher Brett

Approved by: _____
Dr. Grant Brown, Graduate Program Director

Monday, January 23rd, 2023: _____
Dr. Pascale Sicotte, Dean of Faculty of Arts and Science

Abstract

Humanization of Yeast Extracellular Vesicle Biogenesis Machinery to Investigate Functional Evolutionary Conservation

Curtis John Logan, M.Sc.
Concordia University, 2023

Extracellular vesicles (EVs) mediate intercellular communication underlying diverse (patho)physiology, including responses to stress, in all organisms studied from bacteria to yeast to human. However, relatively little is understood about the molecular machinery underpinning fundamental EV biology. The Endosomal Sorting Complex Required for Transport (ESCRT) pathway contributes to the biogenesis of small EV populations called exosomes, including selective loading of luminal and membrane protein cargo. Our group discovered that EVs produced by baker's yeast (*Saccharomyces cerevisiae*) confer thermotolerance. Herein, my aim is to use this powerful model organism to study functional evolutionary conservation of ESCRT-mediated exosome biogenesis. I replaced yeast VPS23 (yeast vacuolar sorting protein 23), a component of ESCRT-I critical for protein cargo selection, with its human orthologue TSG101, a conventional EV biomarker, tagged it to GFP and evaluated if it confers EV cargo loading, biogenesis and bioactivity. After confirming TSG101-GFP protein expression in yeast by Western blot analysis and fluorescence microscopy, I collected EVs and measured their size by Nanoparticle Tracking Analysis (NTA), total protein content by Bradford assay, and GFP-fluorescence using fluorimetry. EVs were also visualized using transmission electron microscopy to assess structural morphology and confirm size. To assess the capacity to restore bioactivity, I collected EVs from conditioned yeast and measured their ability to provide thermotolerance to naïve cells using a methylene blue-based viability assay and light microscopy. Proteomic analysis by mass spectrometry was conducted to identify EV proteins. In all, I found that human Tsg101-GFP seems to localize at sites of exosome biosynthesis within cells, is present in EVs, and replaces most yeast Vps23 functions in exosome biogenesis, suggesting deep evolutionary conservation of ESCRT-mediated EV biology. These studies set the stage for research focused on better understanding the basis of selective protein cargo loading using *S. cerevisiae* as a model.

Acknowledgments

Foremost, I would like to thank my supervisor Dr. Christopher Brett for providing me the opportunity to begin my post-graduate studies in his lab, during the middle of a pandemic. We made the best of these unprecedented times. Your expertise and guidance have helped to prepare me as a researcher. I look forward to seeing what our research accomplishes in the near future.

Furthermore, I thank my committee members Dr. Vincent Martin and Dr. Malcolm Whiteway for their support, feedback, and time commitment throughout the course of this project.

I would like to thank Dr. Chris Law of Concordia University's Centre for Microscopy and Cellular Imaging (CMCI). Your expertise has been imperative to the development and progress of this project.

To Dr. Heng Jiang, the applications specialist of the Centre for Biological Applications of Mass Spectrometry (CBAMS) at Concordia University, I thank you for your eagerness to be involved in the project and much appreciated troubleshooting tips.

I would like to thank Dr. Nooshin Movahed, facility manager of Concordia's Centre for NanoScience Research for their training and assistance with TEM.

To project managers Dr. Nadim Tawil and Laura Montermini at the Canadian Centre for Applied Nanomedicine (McGill University), thank you for your technical continual support in characterizing my lipid nanoparticles. This study's progress would not be where it is without your expertise.

Table of Contents

List of Figures	vii
List of Tables	viii
List of Abbreviations	ix

Chapter 1: Introduction

1.1 Extracellular vesicles and their role in eukaryotic (patho)physiology.....	1
1.2 Extracellular vesicles: Types, origins and biomarkers.....	2
1.3 ESCRT-independent exosome biogenesis	4
1.4 ESCRT-dependant exosome biogenesis	5
1.5 Putative evolutionary conservation of Vps23/TSG101	8
1.6 Exosomes and thermotolerance.....	9
1.7 Thesis objective.....	10

Chapter 2: Materials & Methods

2.1 Yeast strains and reagents.....	17
2.2 Western blot analysis.....	18
2.3 Live cell fluorescence microscopy	18
2.4 Fluorometry to assess EV release.....	19
2.5 Thermotolerance assay.....	19
2.6 EV isolation.....	20
2.7 Fluorometry to detect GFP in isolated EVs	20
2.8 EV sizing by dynamic light scattering (DLS)	21
2.9 Transmission electron microscopy (TEM).....	21
2.10 EV sizing by nanoparticle tracking analysis (NTA).....	21
2.11 Proteomics by liquid chromatography-mass spectrometry (LC-MS).....	22
2.12 Data analysis and presentation.....	22

Chapter 3: Results

3.1 HsTSG101 localizes to sites of ESCRT– dependent exosome biogenesis in <i>S. cerevisiae</i>	24
3.2 EVs released during heat stress contain HsTSG101–GFP	24
3.3 Deleting ScVPS23 or replacing it with HsTSG101 has no effect on exosome size or morphology	25
3.4 EV production increases when HsTSG101 is over–expressed.....	26
3.5 Protein loading and selection into exosomes is disrupted when ScVPS27 is deleted and may be rescued by HsTSG101	26
3.6 TSG101–GFP rescues loss of VPS23 in exosome–mediated thermotolerance	28

Chapter 4: Discussion

4.1 HcTSG101 seems to replace ScVPS23 function in exosome-mediated thermotolerance	38
4.2 ScVps23 contributes to exosome protein selection and sorting for bioactivity	38
4.3 Vps23/TSG101 function in exosome biology seems deeply conserved.....	40
4.4 Conclusion and future directions.....	42
References.....	44

List of Figures

Figure 1. Classes of extracellular vesicles released by cells for intercellular communication.....	12
Figure 2. ESCRT-dependant ILV biogenesis in <i>S. cerevisiae</i>	13
Figure 3. Comparison of ScVps23 and HsTSG101 proteins.....	14
Figure 4. Vps23/TSG101 and exosome-mediated thermotolerance in <i>S. cerevisiae</i>	16
Figure 5. HsTSG101-GFP localizes to ScVPS23-positive sites when over-expressed in <i>S. cerevisiae</i>	30
Figure 6. HsTSG101-GFP is released into extracellular medium during heat stress	31
Figure 7. Transmission electron microscopy confirms EVs are released with or without VPS23/TSG101.....	32
Figure 8. EV size measurements using 3 different methods confirms that ESCRT-I is not involved in exosome formation or release.....	33
Figure 9. HsTSG101-GFP over-expression increases exosome numbers.....	34
Figure 10. LC-MS proteomic characterization of yeast EV cargo proteins.....	35
Figure 11. Humanized yeast exosome bioactivity assay.....	36

List of Tables

Table 1. <i>S. cerevisiae</i> strains used in this study.....	17
--	----

List of Abbreviations

Δ – delta (single gene deletion)
DIC – differential interference contrast
DLS – dynamic light scattering
DNA- deoxyribonucleic acid
ERT – enzyme replacement therapy
ESCRT- endosomal sorting complex required for transport
EV- extracellular vesicle
G418 – Geneticin
GFP – green fluorescent protein
HEK293 – human embryonic kidney cell 293
HSP – heat shock protein
ILV – intraluminal vesicle
LSD – lysosomal storage disorder
MB – methylene blue
MVB – multivesicular body
 μm – micrometers/microns
nm – nanometers
NTA – nanoparticle tracking analysis
OD₆₀₀ – optical density at λ 600nm
PBS – phosphate buffer saline
PM- plasma membrane
PTA - phosphotungstic acid
QELS – quasi-elastic light scattering
RNA -ribonucleic acid
SEM – standard error of the mean
SC -synthetic complete
SC-URA – Synthetic Complete (media) without Uracil
SD – standard deviation
TEM – transmission electron microscopy
TIRF – total internal reflection microscopy
UC -ultracentrifugation
VPS – vacuolar sorting protein
w/v – weight per volume
YPD – yeast peptone dextrose

CHAPTER 1 - INTRODUCTION

1.1 Extracellular vesicles and their roles in eukaryotic (patho)physiology

Extracellular vesicles (EVs) are a heterogeneous class of biologically derived nanoparticles that mediate cell-to-cell communication in all organisms studied from bacteria to yeast to plants to humans (Gill et al., 2019; Chronopoulos & Kalluri., 2020; Bose et al., 2020; Liu et al., 2021). Ranging from 30 nm to > 2 µm in diameter, they are comprised of a spherical lipid bilayer containing membrane proteins that encapsulate luminal cargo including proteins, ribonucleic acids and other bioactive metabolites. Typically, in response to a stimulus, donor cells release EVs into the extracellular environment where they can travel long distances before they are recognized by a selective recipient cell population. Here they deliver their bioactive cargoes by membrane fusion to elicit a specific response (Edgar., 2016). Importantly, luminal cargos encapsulated by EVs are shielded from the external environment, protecting bioactive cargo from nucleases, proteases and fluctuations in pH which may otherwise degrade the biological mediators of intercellular communication. Although first thought to represent inert cellular debris, EVs are beginning to be recognised for their importance in homeostasis, diverse physiological responses, and contributing to pathological states (Wilms et al., 2018; Doyle & Wang., 2019; Yang et al., 2021).

For example, in addition to contributing to tissue development and regeneration, EVs seem to be critical for cell health and survival in response to diverse stressors. For example, when subjected to heat stress, some mammalian cells and yeasts such as *Saccharomyces cerevisiae* release EVs containing heat shock proteins with chaperone activity that help refold misfolded proteins as a potential altruistic means of thermoprotection against future heat stress to ensure survival of the entire cell population (Oliver., 2021). In humans, EVs are thought to mediate cancer cell survival, proliferation and migration for tumour progression and metastasis (Kogure 2020), whereas pathogenic species of yeast such as *Candida* spp. package factors within EVs to dysregulate human host immune responses and promote infection (Karkowska-Kuleta et al., 2020). Further, some membrane-encapsulated viruses like HIV and EBV hijack the host EV biogenesis machinery for synthesis of progeny virions (Garrus et al., 2001; Chua et al., 2007;

Dolnik, 2014). These highlighted EV functions demonstrate broad EV function spanning all phyla suggesting that underlying machinery is likely deeply conserved, but a detailed study of potential orthology has not been conducted.

1.2 Extracellular vesicles: Types, origins and biomarkers

Although the importance of EVs to biology is now apparent, scientists studying complex organisms (e.g. plants, mammals) currently struggle to identify the underlying molecular contributors because of challenges with isolating the EVs responsible from extremely heterogeneous EV populations released from diverse cell types and generated by different EV biogenesis pathways. For example, eukaryotic cells produce at least three major classes of EVs: apoptotic bodies (0.5 – 2 μm) (Borges et al., 2013; Battistelli & Falcieri., 2020), microvesicles (150 – 1200 nm) (Heijnen et al., 1999; Zaborowski et al., 2015), and small EVs (sEVs) or exosomes (30 – 200 nm) (Doyle & Wang., 2019) (**Figure 1**). Common methods of characterizing EVs to help distinguish these different populations are limited to measuring size, density, or electrostatic properties, and identifying vesicle class-specific biomarkers. The electrostatic properties (zeta potential) of lipid nanoparticles in suspension influences particle stability and interactions between particles, including particle aggregation (Midekessa et al., 2020). Further, the internal density of EVs effects particle mass which may be exploited to separate denser EVs from those less dense. Within each class, EVs can vary in their content (protein, RNAs, lipids), physical properties and bioactivity further complicating their study. These properties are known to be dependent on their cellular and sub-cellular origins (i.e. site of biogenesis) and physiological state at the time of EV biogenesis and/or release (e.g. specific loading of bioactive cargo in response to a stimulus). Since EVs are extremely diverse with regards to their biogenesis, physical properties and bioactivity, research regarding fundamental EV biology relies on distinguishing between the subtypes and separating isolated EVs for detailed analyses. For instance, because particles like apoptotic bodies contain different cargo (ie: whole intact organelles) and are considerably larger compared to Exosome-class EVs, studying one class of EVs does not translate to a deeper understanding of those produced by different mechanisms with different intended bioactive responses. The following briefly summarizes unique characteristics of each EV class:

Apoptotic bodies are relatively large EVs (0.5 – 2 μm in diameter) formed by cells undergoing programmed cell death (apoptosis). Apoptotic cells section into multiple compartments which are released as EVs upon fragmentation, or by blebbing of the plasma membrane (Wyllie et al., 1980; They et al., 2009; Hristov et al., 2004; Jiang et al., 2017; Hauser et al., 2017; Santavanond et al., 2021). Apoptotic vesicles range in density from 1.16-1.28g/mL in sucrose gradients (Zhang et al., 2019; Cai et al., 2020). Further, the zeta potential of pure AB membranes is reported to be $\sim 16.6 \pm 0.6$ mV (Dou et al., 2020). Since apoptotic bodies are derived from the components of dying cells, they contain portions of the cytosol, nuclear DNA, histones, and intact organelles. Blunt-ended DNA is used as a biomarker to distinguish predominantly nuclear from cytosolic derived apoptotic bodies (Galleu et al., 2017; Hauser et al., 2017; Gebara et al., 2020). These EVs are primarily involved in mediating clearance of these dying cells by neighbouring live and innate immune cells through phagocytosis; a process though to prevent autoimmune reactivity (Caruso & Poon., 2018; Caruso et al., 2019; Gebara et al., 2020). Otherwise, the expansive role of apoptotic bodies in physiology is not understood.

Microvesicles, also known as ectosomes, are medium-sized EVs (150 – 1200 nm in diameter) believed to be largely derived from outward budding of the plasma membrane via exocytosis (They et al., 2009). In sucrose gradients, high density microvesicles range from 1.25-1.30g/mL, while lower density microvesicles can range from 1.08-1.19g/mL, overlapping with reported exosomes-class particle densities (Zhang et al., 2019). Biomarkers of human microvesicles include CD44, selectins, integrins, annexins or CD40-ligand, which are thought to mediate recognition by specific recipient cell populations and/or regulate cognate downstream signal transduction pathways to drive cellular responses (Mobarrez et al., 2015; Lv et al., 2019; Jeppesen et al., 2019.). For example, microvesicles released by human neutrophils may function in innate anti-microbial responses (Hess et al., 1999) or initiating other inflammatory responses (Cocucci., 2009). Other microvesicles transport oncogenic cargo between cancer cells, including mRNAs and miRNAs which for example promote gene expression underlying multi-drug resistance (Cocucci & Meldolesi., 2009; Menck et al., 2020; Zhu et al., 2021). They are known to be released from other cell types, but their functions are not elucidated, nor is the molecular basis of their biogenesis entirely understood.

Exosomes are small-sized EVs (30 – 200 nm in diameter) believed to be predominantly derived from the endosomal pathway (Yanez-Mo et al., 2015; Doyle & Wang., 2019). Exosomes range in density from 1.13-1.19g/mL in sucrose gradients (Zhang et al., 2019). Further, the zeta potential of EVs suspended in PBS can range from -24.9-21.7 mV, dependant on the ionic strength of the solution (Beit-Yannai et al., 2018). Unlike the other EV classes, small EVs or exosomes are known to be released from all organisms studied spanning all phyla, including yeast and humans. As such, exosomes represent the best EV class to further study potential orthology of conserved mechanisms underlying fundamental EV biology. Exosomes, specifically, are implicated in mediating virulence of many pathogenic fungal species (Rizzo et al., 2021), progression of many human cancer types (Brinton et al., 2015; Yu et al., 2015), and for example, communication in uterine fluid between the maternal endometrium and mammalian embryo and promoting initial stages of human embryogenesis (Machtinger et al., 2016). They also are thought to mediate responses to many environmental stressors, including heat stress, in diverse species and may be responsible for spreading prions underlying pathogenesis of neurodegenerative diseases such as Alzheimer’s or Huntington diseases in humans (Bellingham et al., 2012). Importantly, depending on the donor cell and species, exosomes are thought to be derived by at least two pathways that are known molecular contributors: one that depends on ESCRTs (Endosomal Sorting Complex Required for Transport), and a second that is ESCRT-independent and thought to rely in part on tetraspanins and lipid rafts:

1.3 ESCRT-independent exosome biogenesis

Depending on the organism, ESCRT-independent EV biogenesis mechanisms may utilize tetraspanins or lipid rafts, among others that are not as well characterized: Tetraspanins are multi-pass integral membrane proteins that participate in the biogenesis of some exosome populations. They may produce exosomes either at the endosome or plasma membrane depending on the tetraspanin paralog (van Niel et al., 2011; Toribio et al., 2022). Though the mechanisms are not precisely understood, it is thought that tetraspanins drive changes membrane curvature and deformation required for vesicle formation (Bari et al., 2011). Importantly, tetraspanins themselves are sorted into exosome membranes, and thus are used as conventional biomarkers to identify this EV subtype (e.g. CD63, CD9) (Gutierrez-Vazquez et al., 2013;

Villarroya-Beltri et al., 2014). Tetraspanins are found in all metazoans studied but clear orthologs (based on gene sequence similarity) do not exist in yeast species, although tetraspanin-like proteins have been identified but not studied (Skaar et al., 2015).

Rafts are membrane microdomains enriched with specific lipid populations (see below) that alter biomechanical properties of the bilayer. Depending on lipid content, rafts are implicated in: membrane partitioning required for complex cellular signaling, directing membrane trafficking (Bagnat et al., 2000), regulating organelle contact sites (Ouweneel et al., 2020), and promoting exosome formation (Han et al., 2022). In addition to sterols, which are key components of all lipid rafts, several sphingolipid species enriched in exosomes are implicated in exosome biogenesis, including sphingomyelin and ceramides (Horbay et al., 2022). Given that sphingolipid metabolism is controlled by many overlapping pathways, and different EV populations may contain distinct lipid composition profiles, further investigation into the mechanistic roles of lipids in mammalian exosome biogenesis needs to be explored in depth. However, evidence from studies on mammalian EVs suggests that ceramide production by the sphingomyelinase (SMase) pathway contributes to EV biogenesis (Elsherbini et al., 2021), and that clustered ceramides induce membrane deformation and invagination, requisites for exosome production (Skryabin et al., 2020). Like metazoans, yeast membranes contain lipid rafts, e.g., eisosomes, enriched in sterols and sphingolipids and they are implicated in signaling and trafficking (Bagnat et al., 2000; Guan et al., 2009; Hurst et al., 2020). However, their role in yeast exosome biogenesis has not been explored. Because it remains unclear if tetraspanins and/or lipid rafts contribute to exosome biogenesis in yeast, further study of potential evolutionary conservation is unwarranted at this time.

1.4 ESCRT-dependent exosome biogenesis

While the precise mechanisms are not understood in detail, research suggests that ESCRTs drive biogenesis of some exosome populations in yeast, humans and many other organisms (Katzmann et al., 2001, They et al., 2001; Hanson et al., 2012; Akers et al., 2013; Henne et al., 2013; Kowal et al., 2014.), suggesting they play a conserved role in fundamental EV biology. First discovered in *S. cerevisiae* but found in all eukaryotes, ESCRTs are represented by four multi-protein

complexes named ESCRT-0, -I, -II and -III which function in series for sequestration, selection, sorting and loading of specific protein cargos into developing intraluminal vesicles (ILVs), precursors of exosomes that are released into the cellular surroundings (**Figure 2**). Additionally, ESCRT-III drives alterations in membrane topography (invagination and scission) required for formation of ILVs within the lumen of late endosomes (Katzman et al., 2001; Chu et al., 2006; Curtiss et al., 2007; Henne et al., 2011; Schmidt & Teis., 2012; Gebara et al., 2020). ILVs generated by ESCRTs have two potential fates: they are either sent to lysosomes (or vacuole in yeast) for degradation through the canonical multivesicular body MVB pathway or are released into the extracellular space through fusion of late endosome limiting membranes with the plasma membrane (Grant & Donaldson., 2009). Notably, unlike mammalian cells, fungi and plants have a protective cell wall originally thought to impede exosome release. However, preliminary evidence suggests that pores within cell walls are of sufficient size to accommodate permeation of small EVs like exosomes, but not larger EV classes, from *S. cerevisiae* and other fungi (Zhao et al., 2019; Oliver., 2021). This possibly explains why only exosome-class EVs are implicated in normal fungal EV biology, and further justifies focusing on them to study the basis of potential orthology.

ESCRT-0 initiates protein entry into the exosome biogenesis pathway by binding and sequestering ubiquitinated cargo and subsequently shuttling it to ESCRT-I located on endosome membranes (**Figure 2B**). ESCRT-0 is heterodimeric (containing Vps27 and Hse1) in *S. cerevisiae*, or heterotrimeric in *H. sapiens* (*Stam1*, *Stam2*, *HRS*), with five ubiquitin interacting domains through which it associates with a maximum of five ubiquitin-tagged proteins (Schmidt & Teis., 2012). ESCRT-0 associates with PI3P embedded in the endosomal membrane to facilitate cargo sequestration while perhaps contributing to lipid reordering necessary for vesicle formation (Kim et al., 2018, Schmidt & Teis., 2012). ESCRT-I is a heterotetramer consisting of Vps23, Vps37, Vps28, Mvb1 in *S. cerevisiae* (Hurley & Emr., 2006) and conjugates with ESCRT-0 via interaction with Vps27. It binds ubiquitinated cargo sequestered by ESCRT-0 through a ubiquitin interaction domain in Vps23, the yeast ortholog of human TSG101 a biomarker of human exosomes, which is critical for protein cargo selection (Katzmann et al., 2001; Teo et al., 2004). Thus, it is presumed that Vps27/TSG101 is a critical for determining protein and RNA (via protein carriers) content of newly formed exosomes.

Next in the pathway is ESCRT-II, a heterotrimer comprised of yeast Vps36 (EAP45 in humans), Vps22 (EAP30) and Vps25 (EAP20) (Schmidt & Teis., 2012). Though a Vps28–Vps36 interaction, ESCRT-I binds to ESCRT-II to stabilize transfer of cargo from Vps23/TSG101 to the GLUE domain of Vps36 (**Figure 2B**) (Slagsvold et al., 2005, Hurley & Emr., 2006). When cargo is sorted into ESCRT-II positive microdomains on endosome membranes, Vps25 interacts with ESCRT-III to trigger cargo packaging into newly forming ILVs (Schmidt & Teis., 2012). ESCRT-III is heterotetramer comprised of yeast Vps2 (human CHMP2A-B), Vps20 (CHMP6), Vps23 (CHMP3), and Snf7 (CHAMP4A-C) whose primary function is ensuring cargo loading while driving membrane deformation and eventual scission (Schmidt & Teis., 2012; Buzas et al., 2015). However, final scission, to release cargo protein–laden ILVs into the endosome lumen, requires the activity of two accessory protein complexes: Doa4 a deubiquitylase that removes ubiquitin from protein cargoes immediately before ILV formation to ensure that it is recycled to prevent depletion of cellular ubiquitin pools needed for proteostasis (Hurley & Emr., 2006, Pfitzner et al., 2020). The Vps4 accessory complex comprised of yeast Vps4 (human Vps4a or Vps4b) which is an AAA-ATPase responsible for ATP-dependent disassembly of ESCRTs necessary for final membrane closure and recycling of their components for additional rounds of ILV formation (Henne et al., 2011; Schmidt & Teis., 2012).

Also worth noting is ALIX, an ESCRT accessory protein orthologous to yeast Bro1, is a conventional biomarker of human exosomes (Hoshino et al., 2020). Yeast Bro1 is thought to interact with ESCRT-III, through which it can facilitate ubiquitin –dependent or –independent sorting of proteins into ILVs through a mechanism that bypasses function of earlier ESCRTs, e.g. ESCRT-I but is not understood in detail (Pashkova et al., 2013). Human ALIX can recognize cargo without ubiquitin by, for instance, binding to syntenin which in turn interacts with syndecan– or tetraspanin–bound cargoes (Baietti et al., 2012; Han et al., 2022). These are then supposedly sent directly to ESCRT–III for loading into human exosomes (Han et al., 2022). Whether the yeast ortholog Bro1 performs a similar function is unclear.

The primary goal of my thesis research is to better understand the basis of fundamental EV biology by studying the orthology of underlying mechanisms deeply conserved from yeast to

man representing ~1 billion years of evolutionary divergence. Based on the above, I decided to focus on only ESCRT-derived exosomes because they have been observed in all eukaryotes studied including humans and *S. cerevisiae*. Because the basis of exosome protein and RNA content selection remains enigmatic but critical for understanding EV biology, I chose to study the orthology of ESCRT-I component Vps23/TSG101. Unlike Bro1/ALIX which seems to play roles in cargo selection for multiple, ambiguous exosome biogenesis pathways, there is definitive evidence supporting role of Vps23/TSG101 in ESCRT-mediated exosome biogenesis across species and its role in this process is better understood, permitting interpretation of experimental results and further detailed examination of how it mediates cargo selection.

1.5 Putative evolutionary conservation of Vps23/TSG101

Vps23 from *S. cerevisiae* (ScVps23) and TSG101 from *Homo sapiens* (HsTSG101) are homologous ubiquitin-binding ESCRT-I complex subunits implicated in cargo protein selection and biogenesis of EVs in numerous organisms (Zhao et al., 2019, Oliveira et al., 2010, Gurung et al., 2021). For example, deleting VPS23 negative effects ESCRT-dependent EV biogenesis in fungi (Zhao et al., 2019). Knocking out HsTSG101 results in decreased EV secretion by cultured human cells (HEK293) (Boker et al., 2018). Demonstrating roles in protein selection, deleting ScVPS23 or HsTSG101 mis-localizes proteins typically packaged into ILVs (Li et al., 1999; Babst et al., 2000; Katzmann et al., 2001; Lu et al., 2003). Similar in polypeptide length (380 and 385 amino acids respectively), ScVps23 and HsTSG101 share 52% direct sequence homology (Babst et al., 2000) (**Figure 3A**). Vps23 and TSG101 share several conserved domains essential for function (**Figure 3B and C**). The ubiquitin E2 variant domain (UEV) located at the C-terminus of both Vps23 and TSG101 functions in selecting and binding ubiquitin-tagged proteins (Teo et al., 2004, Katzmann et al., 2001, Bishop et al., 2002, Pornillos et al., 2002). The UEV spans amino acid residues 1-162/1-145 (Vps23/TSG101) (Pornillos et al., 2002; Kostelansky et al., 2006) In the context of exosome biogenesis, the UEV binds ubiquitin-tagged cargo proteins to be loaded into developing ILVs. Further, Vps23 and TSG101 share a conserved proline-rich domain (PRD) spanning residues 162-200/145-217 (Kostelansky et al., 2006; Pornillos et al., 2002) and coiled-coil (COIL) domain 200-322/217-317 (Kostelansky et al., 2006; Chu et al., 2006). The coiled-coil domain functions in supporting ESCRT-I complex assembly in the

endosome (Kostelansky et al., 2007). The C-terminal steadiness box (SB) from residues 322-385/323-390 (Kostelansky et al., 2006; Pornillos et al., 2002) links ESCRT-I and ESCRT-II complexes, enabling exosome cargo selection and sorting (Gill et al., 2007; Kostelansky et al., 2007). Lastly, the PTAP domain contained in TSG101, located between the coiled-coil and steadiness box regions from residues 320-323 (Pornillos et al., 2002) is associated with assembly of HIV virions and may potentially regulate UEV-cargo binding (Lu et al., 2003).

Though ScVps23 and HsTSG101 are widely cited as being evolutionarily conserved, limited research has directly assessed putative functional orthology. The only study to date on potential functional complementation of VPS23 in *S. cerevisiae* found that HsTSG101 may not replace it in the context to plasma membrane protein degradation, i.e. its role in the canonical MVB pathway (Blanco & Lazo., 2003). Given that the directing cargo proteins for degradation is likely distinct from loading them into exosomes, I reason that additional study is required to assess the potential conservation of Vps23/TSG101 function exclusively in context to EV biology.

1.6 Exosomes and thermotolerance

In all organisms examined, EVs seem to contribute to physiological responses to external stressors including hypoxia, oxidative stress and heat stress (Eldh et al., 2010; Shao et al., 2018; Rodrigues et al., 2019; Oliver., 2021). These stimuli are thought to potentially drive preferential enrichment of protein cargos within EVs that function in specific stress response pathways. These are then shared between cells to help ensure population survival (Bister et al., 2020; Qi et al., 2021). For example, mammalian cells preferentially load heat shock proteins (HSPs) into EVs when confronted with heat stress (that misfolds proteins) or other proteotoxic stressors (Gebremedhn et al., 2020; Regimbeau et al., 2022). Depletion of EVs from heat stressed bovine mammary epithelial cell cultures, for example, increases apoptosis, oxidative damage, and mitochondrial damage, demonstrating that these EVs promote cell survival (Wang et al., 2022). The HSP Hsp90, a key chaperone protein, can directly interact with TSG101 which likely promotes loading into exosomes, as well as offering a mechanism for loading other soluble, cytoplasmic proteins through binding Hsp90. This interaction also increases TSG101 stability,

supposedly increasing ILV biogenesis (Giordano et al., 2019; Regimbeau et al., 2022). Overall, given that TSG101 is able to directly interact with heat shock proteins destined for packaging within ILVs, these particles later released as EV are likely to primarily function in thermoprotective response to heat stress.

Although EV biology is understudied in *S. cerevisiae*, it was recently discovered that ESCRT-derived exosomes play an important role in thermotolerance (Oliver., 2021). This is consistent with studies on human cells suggesting that the underlying mechanisms are conserved. In support, the HSPs Ssa2, an Hsp70 ortholog, and Hsc82, an Hsp90 ortholog, were implicated as being critical EV components that mediate the observed response (Oliver., 2021). While EVs collected after heat stress elicited thermoprotection, EVs collected after osmotic stress did not, supporting the hypothesis that cargo protein selection is likely stressor-specific (Oliver., 2021). Exosomes collected from monoclonal *S. cerevisiae* during a relatively short period of heat stress (30 minutes at 42°C) were relatively homogenous, mitigating issues associated with EV heterogeneity, one of the greatest challenges in the field. Given that this effect seems conserved, is mediated by ESCRT-derived exosomes, and requires proper protein cargo selection, I reasoned that exosome-mediated thermotolerance in *S. cerevisiae* is an exceptional model to investigate potential orthology of ESCRT-I component Vps23/TSG101.

1.7 Thesis Objective

The importance of EVs and exosomes to (patho)physiology is now evident, but the mechanisms underpinning many aspects of fundamental EV biology, including the basis of protein cargo selection, are not understood in detail. Although it is established that ESCRTs mediate selective cargo protein loading and formation of ILVs, nearly all published studies focus on their role in integral membrane protein degradation through the canonical MVB pathway whereas their function in exosome biology is unresolved. Moreover, it remains unclear how ESCRT-I selects some soluble and integral membrane proteins to be loaded into ILVs destined to be secreted as exosomes, as compared to other proteins loaded into ILVs destined for degradation by lysosomes. Given that (1) *S. cerevisiae* has been used with great success to uncover the molecular basis of many fundamental processes underlying eukaryotic cell biology (Galao et al.,

2007) 2) genes encoding ESCRT components are conserved among all eukaryotes and (3) ESCRT-derived exosomes are the only EV type that seem to function in organisms from yeast to man, I reasoned that studying the orthology of Vps23/TSG101, a key component of ESCRT-I required for exosome cargo protein selection, offers an exceptional opportunity to better understand the basis of EV biology.

To this end, I hypothesize that HsTSG101 can replace the function(s) of ScVPS23 in exosome-mediated thermotolerance in *S. cerevisiae* (**Figure 4**). To test this hypothesis, I humanized yeast by transforming VPS23 knockout cells (*vps23Δ*) with a plasmid containing HsTSG101. To accommodate detection within live cells and exosomes, the human ortholog was tagged with GFP at its C-terminus. I then determined if HsTSG101-GFP expression rescued effects of deleting ScVPS23 on exosome numbers, size, morphology, protein content and bioactivity in response to heat stress.

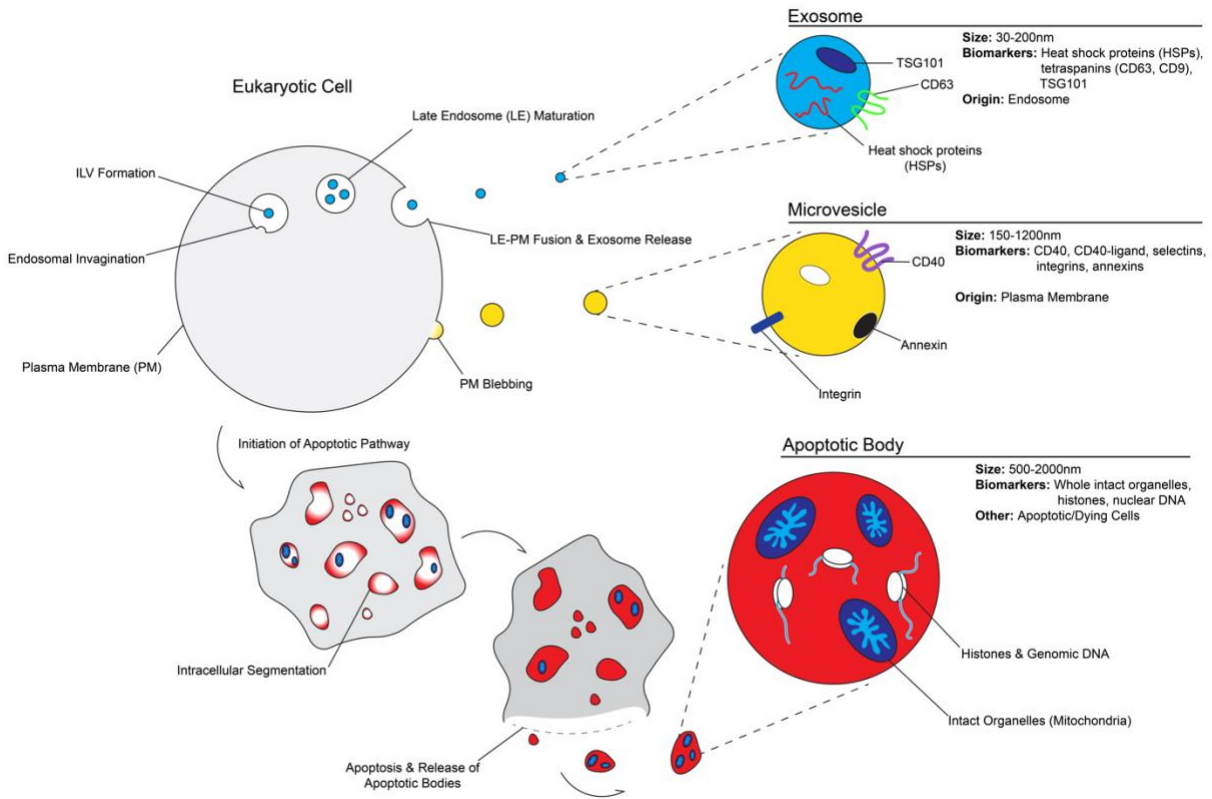


Figure 1. Classes of extracellular vesicles released by cells for intercellular communication

Eukaryotic cells produce three main classes of extracellular vesicles (EVs): exosomes, microvesicles and apoptotic bodies. EV production can be triggered by different external stimuli, including heat stress. Exosomes are believed to be produced via membranous invaginations of the endosome, generating ILVs later released as exosomes upon fusion of the late endosome and plasma membranes. Microvesicles form from blebbing of the plasma membrane, while apoptotic bodies are generated from whole cells undergoing apoptosis (programmed cell death). EV cargo is delivered to the cytosol of recipient cells via back-fusion upon endocytosis of EVs, eliciting a wide range of physiological responses dependant on the stress driving EV production and the class of EVs internalized.

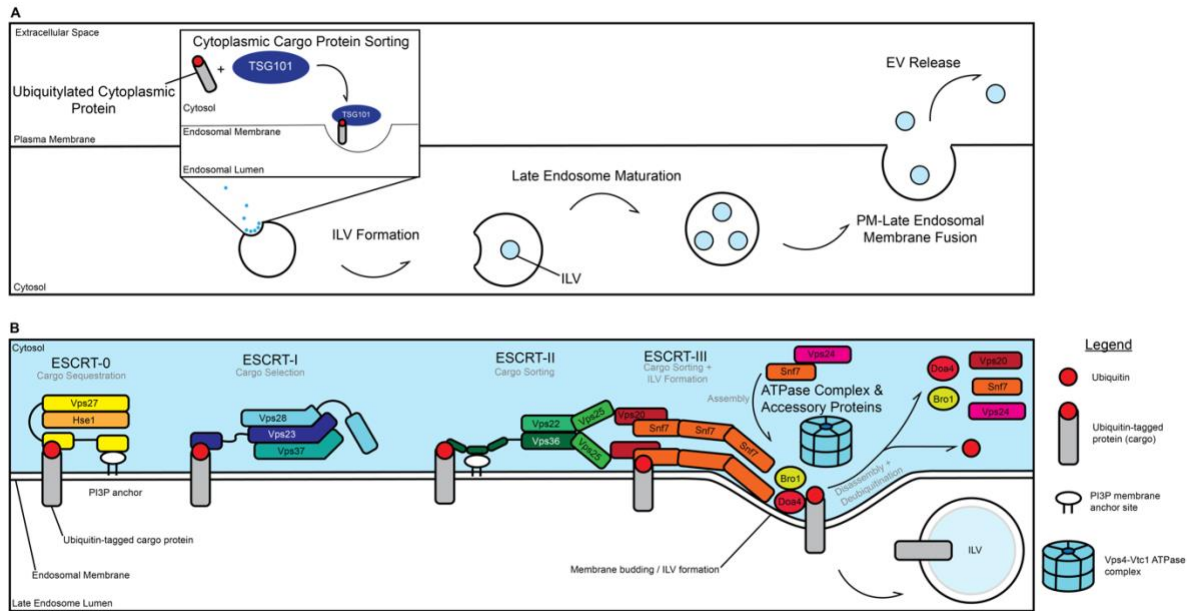


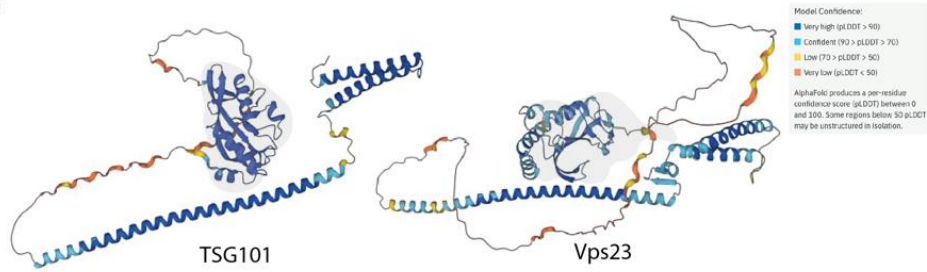
Figure 2. ESCRT-dependent ILV biogenesis in *S. cerevisiae*

(A) ESCRTs are recruited to the cytoplasmic leaflet of endosome membranes within eukaryotic cells where they select and load membrane and cytoplasmic proteins into intraluminal vesicles (ILVs). Multiple rounds of ILV formation form a mature multivesicular body (MVB). MVBs have two fates: they fuse with lysosomes exposing protein-laden to acid hydrolases for degradation, or they fuse with the plasma membrane releasing ILVs as exosome into the extracellular space. (B) ESCRT-0 sequesters potential cargo proteins at the late endosome membrane via ubiquitin-dependant interactions. ESCRT-I retrieves proteins from ESCRT-0, selecting cargo for transfer to ESCRT-II for cargo sorting. ESCRT-III loads cargo protein sorted by ESCRT-II into newly forming ILVs. ESCRT-III also forms filaments that deform and cleave the endosome lipid bilayer to generate ILVs. Immediately prior to ILV release into the lumen, ESCRTs are disassembled by Vps4 AAA-ATPase and cargo proteins are deubiquitinated by Doa4. Bro1 may bypass early ESCRTs and sort proteins into ILVs by directly interacting with ESCRT-III. Adapted from (Slagsvold et al., 2006; Saksena et al., 2007; Schmidt et al., 2012).

A

TSG101	1	-----MAVSE---SOLKRMVSKYKVRD--LTVRETVNVITLYKDLKPFVL	39
Vps23	1	MSANGKLSVPEAVVNWLFKVIQPI-YNDGRITFHDSLALLDNFHSLSRPT	49
TSG101	40	DSYVFNDCSSRELMNLTCTIPVPPYRGNT-YNIPTCLWLLDTYFYNPFIC-	87
Vps23	50	RVFTHSDGTPQLLSIYCTISTGEDSSPFSIPVIMWVPSMYFVKPFIS	99
TSG101	88	-----FVKPSSMTIKTKCHKVDANGKIYLFYLHEFKHPQSDLLGLIQVMI	132
Vps23	100	INLENFDMNIISSSLPIQEYIDSNQWIALPILHCWDPAAMNLTMVVQELM	149
TSG101	133	VVFGDEPPVFSRIFISASYPPYQATGPPNTSYMEGMPGGISPYPSGYPPNF	182
Vps23	150	SLL-HEPFDQAESLPPKPNITLQQEONTPLLPKPK--SPHLK--PPEL	194
TSG101	183	SGYPGCPYPPGGYPATISSQYPSQPPVTVGPSRD-----GTISEDT	225
Vps23	195	-----PPPPQPPASNALDLMMDN-TPISPTNHHEMLQNLQTVVNEL	235
TSG101	226	IASLISA VSDKLRW---MKEEMDRQAQELNALKRTEEDLKGHQKLEE	272
Vps23	236	YRED-VDYVADKILTRQIVMQESIARFH-EIATDKNH--LRAVEQALEQ	281
TSG101	273	MVTRLDCEVAEVDKNIPELLKKDEELSSALEKMENOSENNDDIVILPTA	322
Vps23	282	TMHSLNAGIDVLTAN---RAKVQFSSST---SHVDBEDVNSIAWAKT	322
TSG101	323	PLYKQILNLYAEEENATEDTIFYLGEALRRGVLDLVFLKHVRLLSRKQEQ	372
Vps23	323	DGLNQLYNLVAQDYALDTIECSRMLHRGTIPLDTFVKQGRELARQQEL	372
TSG101	373	LRALMCKARKTAGLSDLY	390
Vps23	373	VRWHIQ--RITSPLS---	385

B



C

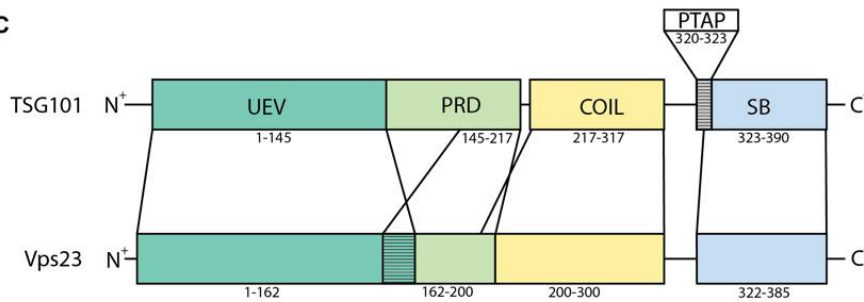


Figure 3. Comparison of ScVps23 and HsTSG101 proteins

(A) Pairwise alignment of amino acid sequences of Vps23 from *S. cerevisiae* and TSG101 from *H. sapiens*. Residues highlighted in blue indicate identical or strongly similar residue consensus between species. Here, ‘strongly similar’ refers to amino acids having similar physical and chemical properties influencing protein structure. Non-conserved residues are described as ‘weakly similar’. Amino acid sequence alignment of TSG101 **(B)** AlphaFold predicted 3D protein structures of Vps23 and TSG101 (Jumper et al., 2020; Varadi et al., 2021.) **(C)** Map of peptide domains and motifs thought to be responsible for Vps23 or TSG101 function in exosome biogenesis. Adapted from REF (Chu et al., 2006; Pornillos et al., 2002).

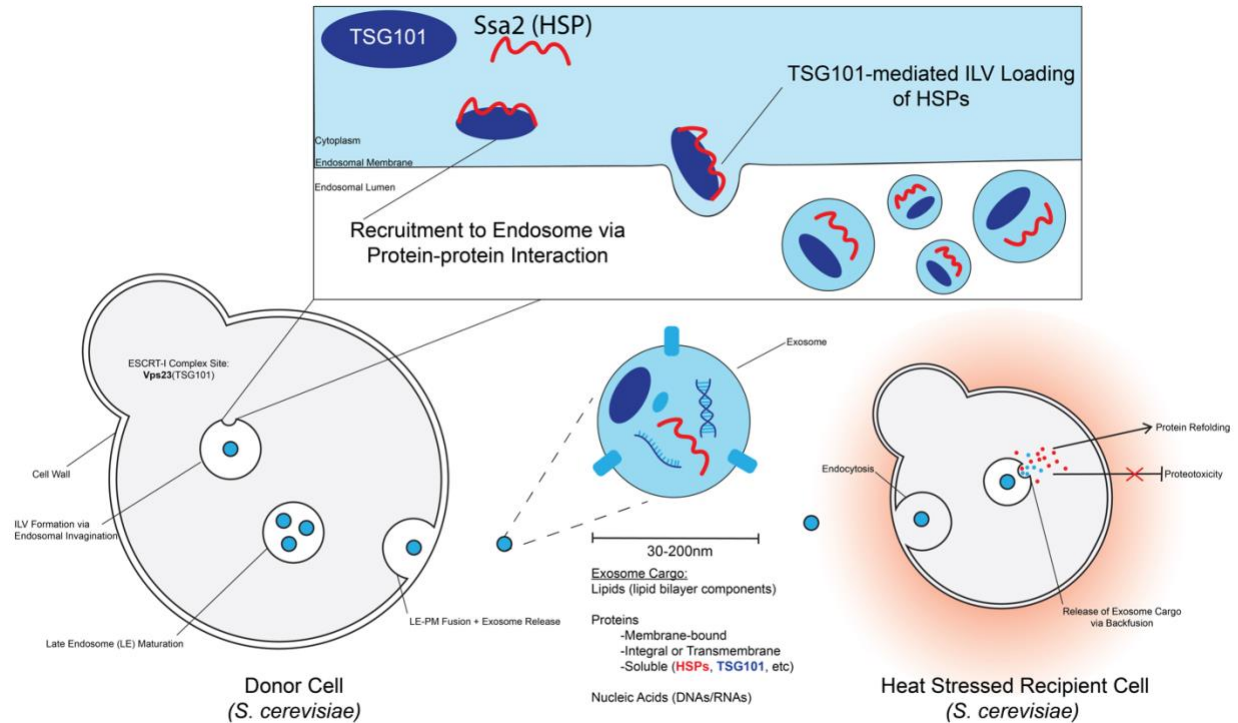


Figure 4. Vps23/TSG101 and exosome-mediated thermotolerance in *S. cerevisiae*

I hypothesize that ScVps23 contributes to exosome-mediated thermotolerance in yeast and that HsTSG101 can replace its function: Vps23/TSG101 in ESCRT-I should localize to endosomes where it is likely selects bioactive cargo proteins, e.g. Ssa2 and Hsc82, that are loaded into exosomes when cells are triggered by heat stress. These exosomes should average between 30-200 nm in diameter when released and contain the exosome biomarker TSG101 if generated by ESCRTs. Recipient cells should take up the exosomes by endocytosis and release their cargoes to confer to thermotolerance.

CHAPTER 2 – MATERIALS AND METHODS

2.1 Yeast strains and reagents

All *Saccharomyces cerevisiae* strains used in this study are listed in **Table 1**. Reagents for yeast growth, EV isolation and imaging or biochemical assays were purchased from Thermo Scientific, BioShop Canada Inc., Invitrogen and Sigma-Aldrich. Mat- α yeast deletion clones used are from the complete set purchased from Invitrogen Corp. (Cat# 95401.H2; Carlsbad, USA). All reagents for molecular biology (enzymes, polymerases, ligases) were purchased from New England Biolabs (Ipswich, USA). Biochemical and yeast growth reagents were purchased from Sigma- Aldrich (Oakville, Canada), Thermo-Fisher Scientific (Burlington, Canada), or BioShop Canada Inc (Burlington, Canada). Recombinant rabbit IgG raised against GFP (B2) was purchased from Abcam (Cat# ab290, Cat# ab113688; Toronto, Canada) and rabbit IgG against G6PDH was purchased Sigma-Aldrich (Cat# A9521). Horseradish peroxidase-labeled affinity purified IgG to rabbit was purchased from SeraCare (Cat# 5450-0010; Milford, USA).

Table 1. *S. cerevisiae* strains used in this study

Strain	Genotype	Source
BY4741	<i>MATa his3-Δ1 leu2-Δ0 met15- Δ0 ura3-Δ0</i>	Huh et al., 2003
<i>vps23Δ</i>	BY4741, <i>vps23Δ:G418</i>	Invitrogen Corp.
<i>vps23Δ::TSG101-GFP</i>	BY4741, <i>vps23Δ:G418, URA3</i>	This study
BY4741:: <i>TSG101-GFP</i>	<i>BY4741, -URA3</i>	This study
BY4741:: <i>Vps23-RFP</i>	<i>BY4741, -LEU2</i>	This study
<i>vps23Δ::Vps23-RFP</i>	BY4741, <i>vps23Δ:G418, -LEU2</i>	This study
<i>vps23Δ::TSG101-GFP</i> Vps23-RFP	BY4741, <i>vps23Δ:G418, -LEU2, - URA3</i>	This study
BY4741:: <i>TSG101-GFP</i> Vps23-RFP	BY4741, <i>-LEU2, -URA3</i>	This study

2.2 Western blot analysis

Yeast cultures were grown in 5 mL selective medium for 17 hours at 30°C in a shaking incubator. 1 OD_{600 nm}/mL unit of cells were then collected by centrifugation (3,000 x g, 5 minutes). Pellets were resuspended in 10% TCA and incubated on ice for 1 hour, then washed with 0.1% TCA. The washed pellet was resuspended in boiling buffer (1.5 M Tris, 0.5 M EDTA, 10 % SDS), vortexed and heated at 65°C for 30 minutes. Urea buffer was added and samples were vortexed and heated again. Protein extracts (10 µL) were then separated by 10% SDS-PAGE and transferred to nitrocellulose membranes. Membranes were blocked in 10 ml 5% skim milk or 3% BSA in PBST prior to incubation with primary anti-GFP, anti-TSG101 or anti-G6PDH antibodies (1:1000 dilution) for 1 hour at room temperature. Membranes were washed 5 times with in PBST for 5 minutes and then incubated for 45 minutes at room temperature with secondary goat anti-mouse or goat anti-rabbit antibodies (1:10,000 dilution). Membranes were then washed 5 times again with PBST. Chemiluminescence was then imaged using a GE Amersham Imager 600 (GE Health Care, Piscataway, USA). Blots shown are best representatives of 3 biological replicates.

2.3 Live-cell fluorescence microscopy

Yeast cultures (5 mL) were grown in selective media at 30°C for 17 hours in a shaking incubator. 5 OD_{600nm} units of cells were harvested by centrifugation (3,000 x g, 5 minutes), washed, and resuspended in 100 µL of SC media. 10 µL of resuspended cells were transferred to glass slides, covered with glass coverslips, and imaged with a Nikon Eclipse TiE inverted microscope equipped with a motorized TIRF (Total Internal Reflection Fluorescence) illumination unit, Photometrics Evolve 512 EMCCD (Electron Multiplying Charge Coupled Device) camera, Nikon CFI ApoTIRF 1.49 NA × 100 objective lens, and 488nm or 561nm 50mW solid-state lasers operated with Nikon Elements software. At least two biological replicates were conducted for each strain.

2.4 Fluorometry to assess EV release

Yeast cultures were grown in 15 mL of selective growth media at 30°C for 17 hours in a shaking incubator. Aliquots containing 10 OD_{600 nm} units of yeast cells were pelleted by centrifugation (3,000 x g for 5 minutes), washed twice with 1 mL 1X PBS, and resuspended in 500 µL 1X PBS. Resuspended cells were then incubated at 30°C (control) or 42°C (thermotolerance conditioning) for up to 30 minutes. At 0 (no incubation), 10, 20 and 30 minutes, cells were pelleted by centrifugation (10,000 x g for 5 minutes) and supernatants were filtered (0.22 µm) to collect EVs. 100 µL of filtrates were then transferred to a conical-bottom black 96-well plate and GFP fluorescence intensity was measured using a multimode plate reader (BioTek Synergy H1). Data shown were normalized to values observed at 30°C (control). At least 3 biological replicates were conducted for each strain studied.

2.5 Thermotolerance assay

Yeast cultures were grown in 15 mL of selective media for 17 hours at 30°C in a shaking incubator. Aliquots of cells (each 1 OD_{600nm} unit) were then collected by centrifugation (3,000 x g, 5 minutes), washed twice with SC medium, and resuspended in 100 µL SC medium. Samples were then incubated at 30°C for 30 minutes (control). Cells were then either incubated at 42°C for 30 minutes (for thermotolerance conditioning) or incubated at 30°C for 30 minutes in the presence of 0.10 or 0.25 µg exosomes collected from other cultures after heat stress. After recovery (30°C for 30 minutes), cells were then incubated at 50°C for 30 minutes eliciting an extreme heat stress. Samples were then immediately placed on ice. Prior to imaging, 100 µL of 0.1% (w/v) methylene blue (MB) solution was added to cells which were then incubated at room temperature for 5 minutes. 10 µL of stained cells were transferred to glass slides, covered with glass coverslips, and imaged using a Nikon Eclipse TiE inverted epifluorescence microscope via 40 × objective lens (Nikon CFI Plan Apo Lambda 0.95 NA), DIC optics, and a color CMOS digital camera (Nikon DsRi2, 4908 × 3264 pixels). To assess culture viability, micrographs were used to count live (MB⁻) and dead (MB⁺) cell using ImageJ software. At least 5 technical replicates and 3 biological replicates were conducted for each condition, and > 300 cells were analyzed for each condition tested.

2.6 EV isolation

Yeast seed cultures were grown in 15 mL of selective medium for 8 hours at 30°C in a shaking incubator. These were then used to inoculate three 1 L cultures (3 L total for each strain) grown for ~ 17 hours at 30°C in a shaking incubator. Cells were then collected by centrifugation (3,000 x g, 15 minutes), pooled and washed 3 times with sterile 1X PBS. Cell pellets were then incubated at 42°C for 15 minutes, resuspended in 25 mL sterile 1X PBS, and incubated again at 42°C for 15 minutes for thermotolerance conditioning. Cultures were then immediately placed on ice and cells were pelleted by centrifugation (5000 x g, 15 minutes) at 4°C. The supernatant containing EVs was transferred to clean tubes and subjected to centrifugation at 15,000 x g for 15 minutes at 4°C to remove large cellular debris. Cleared supernatants were then filtered (0.22 µm) prior to use.

For TEM, NTA and proteomic analysis by mass spectrometry, EV samples (15 mL) were transferred to 100 kDa Amicon ultrafiltration units and centrifuged (twice) at 3,000 x g for 15 minutes. Concentrated EV samples were transferred to fresh tubes and preliminarily assessed by fluorimetry (to detect TSG101–GFP), Bradford assay (to measure protein content), and DLS (to measure size) – as quality control measures – and stored at 4°C prior to conducting NTA. For thermotolerance assays, EV samples (25 mL) were loaded into 12.5 mL ultracentrifuge tubes and subjected to centrifugation at 100,000 x g for 1 hour at 4°C. Pellets containing EVs were resuspended in 100 µL ice–cold sterile 1X PBS. Quality control assessment was immediately performed and samples were stored at 4°C until use.

2.7 Fluorometry to detect GFP in isolated EVs

EVs collected by filtration (100 µL) were transferred to a black 96-well conical-bottom microtiter plate and GFP fluorescence ($\lambda_{\text{ex}} = 488 \text{ nm}$; $\lambda_{\text{em}} = 510 \text{ nm}$) was measured using a fluorescence multimode plate reader (BioTek Synergy H1).

2.8 EV sizing by dynamic light scattering (DLS)

To measure particle size by DLS, EV collected by ultracentrifugation were diluted 1:10 (10 μ L EVs added to 90 μ L 1X PBS) and filtered using 0.22 μ m syringe filter units. 20 μ L was then loaded into a QS 1.50 mm quartz cuvette and measurement were acquired using a DynaPro-Microsampler and analyzed using Dynamics 6.7.7.9 software (Wyatt Technology). Particle size analysis was conducted at 4°C and 85% laser power. Average diameter was measured from 100 consecutive acquisitions per sample. At least 3 technical replicates were conducted for each sample, and at least 3 biological replicates were conducted for each strain examined.

2.9 Transmission electron microscopy (TEM)

EVs collected by ultracentrifugation were first fixed by adding (1:1) 2.5 % glutaraldehyde in 0.1 M sodium cacodylate buffer. 5 μ L of fixed EVs were dropcast onto glow discharged carbon-coated grids and were allowed to adsorb onto grids for 5 minutes at room temperature. Grid were then washed twice with glycine solution to remove excess fixative. Grids were then wash four time with ultrapure MilliQ water to remove excess glycine. Mounted EVs were negative stained with 1% phosphotungstic acid (PTA) for 1 minute. Excess PTA was removed using filter paper and grids were airdried for 1 hour at room temperature. Fixed and mounted samples were then imaged using a Talos L120C transmission electron microscope. Micrographs of 4090 x 4096 pixel dimension were acquired using settings HT(80-120kV), Exposure (1-5 sec), Mag(13,500 – 45,000 X).

2.10 EV sizing by nanoparticle tracking analysis (NTA)

EVs collected by ultrafiltration and sample particle size and concentration was measured using ZetaView or NanoSight instruments. 1 mL of diluted or undiluted sample was filtered (0.22 μ m) and slowly injected until conditions appeared optimal for measurement acquisition. ZetaView instrument settings were as follows: Temperature (~25°C), laser λ (488nm), Filter λ (scatter) Sens (85), Shutter (100), FR (30), Trace length (15).

2.11 Proteomics by liquid chromatography-mass spectrometry (LC-MS)

For proteomic analysis by LS-MS, EVs were isolated from WT, *vps23Δ* or *vps23Δ::TSG101-GFP* by centrifugal ultrafiltration. EV proteins were resolved by SDS-PAGE, gels were stained with Coomassie Brilliant Blue R-250 (BioShop) to visualize protein samples that were then excised. Gel pieces were then added to 200 μ L 50 mM NH_4HCO_3 containing 10 mM dithiothreitol (DTT; a reducing agent) and incubated for 30 minutes at room temperature. A total volume of 200 μ L 50 mM NH_4HCO_3 containing 50 mM iodoacetamide (for alkylation) was added, and the sample was incubated for 30 minutes at room temperature. Reduced and alkylated gel pieces were then washed at room temperature with 50 mM NH_4HCO_3 for 15 minutes, 25 mM NH_4HCO_3 containing 5% acetonitrile (ACN) for 15 minutes, 25mM NH_4HCO_3 containing 50% ACN for 30 minutes (twice), and 100% ACN for 10 minutes. Gel pieces were then dried at 43°C by Speed Vac (Savant) and rehydrated in 25 mM NH_4HCO_3 containing porcine pancreas trypsin (Sigma Aldrich) for 12 – 14 hours at 30°C. Digested peptides were then extracted by incubating samples with 60% ACN containing 0.5% formic acid. Extracted peptides were dried at 43°C by Speed Vac and stored at -20°C. Samples were resuspended in 10 μ L 5% methanol containing 0.1% trifluoroacetic acid (TFA) and analyzed by LC-MS using a Thermo LTQ Orbitrap Velos mass spectrometer with a nano-spray ion source configured with Thermo EASY nLC II liquid chromatography system at the Centre for Biological Applications of Mass Spectrometry (CBAMS) at Concordia University. At least two biological replicates were conducted per condition.

2.12 Data analysis and presentation

Images acquired from Western blot chemiluminescence were processed using Adobe Photoshop CC software. Cell viability measurements of micrographs collected for intrinsic thermotolerance conditioning and humanized EV bioactivity assays were manually quantified using the ImageJ Cell Counter plugin. Micrographs were quantified by counting the total number of live cells and the total number of dead cells. Data generated from ZetaView NTA analysis were analysed using ParticleMetrix ZetaView software (version 8.0.5.14 SP7) and excel. Global pairwise alignment of ScVps23 and HsTSG101 amino acid sequences was conducted via EMBL-EBI, using a

Vps23 sequence from the Saccharomyces Genome Database (SGD ID: S000000514) (Madeira et al., 2022) and UniProt sequence for TSG101 (*H. sapiens*) (The UniProt Consortium., 2021).

Mass spectrometry data was analyzed using Proteome Discoverer 2.4 software (Thermo Scientific). Reported peptides and proteins have a false discovery rate < 1%. Results were compared with the *S. cerevisiae* proteome to identify which yeast proteins are present in samples. Bar graphs and Venn diagrams indicating shared protein identity or relative abundance were generated using excel. Data are reported as mean \pm S.E.M. Comparisons were calculated using Student two-tailed t-test; *P*- values are indicated and $P \leq 0.05$ suggests significant differences. An experiment is defined as a sample prepared from a separate yeast culture on different days. Micrographs were processed using ImageJ and Adobe Photoshop CC software.

CHAPTER 3 – RESULTS

3.1 HsTSG101 localizes to sites of ESCRT– dependent exosome biogenesis in *S. cerevisiae*

To replace ScVPS23 with HsTSG101, I generated a VPS23 knock out *S. cerevisiae* strain that expresses human TSG101 tagged to GFP at its C-terminus. *vps23Δ* yeast were transformed with a 2 μ (high–copy) plasmid with URA3 auxotrophic selection containing HsTSG101 C-terminally fused to GFP behind a strong TDH3 promoter (**Figure 5A**). I selected this strategy that ectopically over–expresses HsTSG101 to ensure that resulting protein levels were sufficient to replace ScVps23 function if the human ortholog is not entirely compatible. Western blot analysis of whole cell lysates using anti-GFP or anti-TSG101 antibodies confirmed the presence of HsTSG101–GFP in *vps23Δ::TSG101-GFP* yeast cells (**Figure 5B**). I next visualized these cells using fluorescent microscopy to assess the location of HsTSG101-GFP (Figure 5C). After confirming that untransformed cells (wild type, *vps23Δ*) did not show background fluorescence, I found that TSG101–GFP primarily localizes to punctate like structures within these strains. I observed similar patterns within live cells when I over–expressed ScVPS23 C-terminally tagged to RFP in wild type or *vps23Δ* cells. Co-expression of yeast (VPS23–RFP) and human (TSG101–GFP) orthologs in the same cells showed that their locations overlapped although the pattern of expression seemed to be more restricted compared to when each was expressed alone (**Figure 5C**). All things considered, I conclude that HsTSG101 seems to localize at the same sites as ScVps23, likely representing endosomes where exosomes are made within cells.

3.2 EVs released during thermotolerance conditioning contain HsTSG101–GFP

Although it is unresolved if ScVps23 is present within exosomes, extensive evidence suggests that HsTSG101 decorates human exosomes, and thus is often used as a biomarker of this EV subclass (Conde-Vancells et al, 2008). Thus, I hypothesized that if TSG101–GFP is contributing to exosome biogenesis in yeast, then it should be present in exosomes shown to be released during mild heat stress (42°C for 30 minutes) for thermotolerance conditioning (Oliver, 2021). To test this hypothesis, I collected the extracellular medium and filtered it to crudely purify EVs from *vps23Δ::TSG101-GFP* cells before (0) or 10, 20 or 30 minutes after mild heat stress and

determined if these samples contained TSG101–GFP using fluorometry (**Figure 6**). I found that GFP fluorescence within these samples increased over time, suggesting that HsTSG101 was released into the extracellular medium, presumably within exosomes, during mild heat stress, consistent with results from mammalian studies.

3.3 Deleting ScVPS23 or replacing it with HsTSG101 has little effect on exosome size or morphology

ESCRT–I, and its components Vps23/TSG101, are implicated in ILV protein selection but not vesicle biogenesis (Katzmann et al., 2001; Teo et al., 2004). Thus, although exosome protein content may change, the morphology and size of the EVs produced in the presence or absence of ScVPS23 or HsTSG101 should be indistinguishable from wild type. To confirm, I first visualized EV samples collected by filtration from yeast cells after thermotolerance conditioning (42°C for 30 minutes) using transmission electron microscopy (TEM; **Figure 7**). I found that samples collected from wild type, *vps23Δ* and *vps23Δ::TSG101-GFP* cells all contained particles resembling vesicles with intact membranes and diameters under approximately 170 nm, hallmarks of exosomes. This confirmed the presence of exosomes in extracellular fractions from all strains and confirms that deleting ScVPS23 or replacing it with HsTSG101 has no effect on exosome morphology as expected.

Next, to measure the size of EVs released from these yeast strains, I used three methods to meet MISEV guidelines established by researchers in this field (They et al., 2018; Poupardin et al., 2021) because each has benefits and shortcomings: dynamic light scattering (DLS; **Figure 8A**) and nanoparticle tracking analysis (NTA) by NanoSight (**Figure 8B**) or ZetaView (**Figure 8C and D**) instruments. As expected, mean particle (EV) size measurements for samples derived from each strain slightly differed based on biases associated with each technology used. However, I found that EVs released from wild type cells were on average 130 – 145 nm in diameter, confirming that they represent exosomes consistent with a previous report (Oliver, 2021). Deleting VPS23 had no effect on EV size when measured using NTA but DLS showed a potential reduction in size. Regardless, average diameters recorded from all methods between 90 to 140 nm suggested that exosomes continued to be released from *vps23Δ* cells during heat stress

as predicted. Replacing ScVPS23 with HsTSG101 seemed to increase EV size based on NTA but not DLS, but again mean diameters recorded (125 to 175 nm) confirmed that EVs were released and sizes suggested that they were exosomes. Further examination of particle (EV) size distributions by ZetaView analysis confirm that all particle released from these strains were relatively small, representing only the exosome EV subpopulation (**Figure 8D**). Thus, I conclude that deleting ScVPS23 or replacing it with HsTSG101 does not affect formation and release of exosomes from yeast cells as expected.

3.4 Exosome production increases when HsTSG101 is over-expressed in *vps23Δ* cells

One advantage of ZetaView NTA is that it also accurately counts the number of particles (or EVs) in samples. I used it to test possible effects of HsTSG101 over-expression on exosome biogenesis and found that 1 OD_{600nm} unit of *vps23Δ::HsTSG101-GFP* cells released 3.79×10^6 particles, nearly 7 times more than *vps23Δ* and 14 times more than wild type cells, after thermotolerance conditioning (**Figure 9A**). When considering the size distribution of these particles (**Figure 9B**), I found that most particles are EVs with diameters between 65 – 265 nm confirming that they are likely exosomes. Thus, it seems that over-expressing HsTSG101-GFP in place of ScVPS23 increases exosome biogenesis and release. However, whether this is due to its abnormally high-expression levels or enhanced activity of the HsTSG101 protein compared to ScVps23 is unclear.

3.5 Disruption of exosome protein selection and loading caused by deleting ScVPS23 may be rescued by HsTSG101

Because ESCRT-I is implicated in exosome protein selection, I hypothesized that deleting ScVPS23, a component of ESCRT-I, should disrupt this processes and HsTSG101 should rescue defects if it is functionally orthologous. To test this hypothesis, I measured total protein content of exosome fractions collected by ultrafiltration from yeast after thermotolerance conditioning by Bradford assay (**Figure 10A**). Compared to wild type cells, exosomes released by *vps23Δ* cells had significantly more protein content per vesicle, when vesicle number measured by ZetaView NTA were taken into account (see **Figure 9A**). This suggested that deleting VPS23 disrupted

protein selection prior to loading into exosomes as expected. Total protein content of exosomes released by *vps23Δ::TSG101*–GFP cells was similar to wild type (**Figure 10A**), suggesting that HsTSG101 may in part rescue loss of ScVps23 function.

Next, to determine effects of VPS23 deletion and HsTSG101 replacement on exosome protein identity, I conducted proteomic analysis by mass spectrometry on exosomes collected by ultracentrifugation after thermotolerance conditioning. I predicted that exosome protein identity is altered in *vps23Δ* compared to wild type cells and should be corrected, at least in part, by HsTSG101. I pooled data from three biological replicates and found that of the 361 proteins identified (i.e. with at least 1 unique peptide found) in wild type exosomes, 333 continued to be present in exosomes from *vps23Δ* cells (**Figure 10B**). However, mutant exosomes contained an additional 163 proteins (496 total) indicating that only 67% of proteins identified were similar to wild type, consistent with a defect in protein selection. Over-expression of HsTSG101 in *vps23Δ* cells seemed to partially restore exosome protein identity whereby 8 proteins missing from *vps23Δ* exosomes compared to wild type reappeared in exosomes from these cells (i.e. these proteins were exclusively found in exosomes from wild type and *vps23Δ::TSG101*–GFP cells; **Figure 10B**). In support, 405 total proteins were identified and 75% were similar to wild type exosomes, compared to 67% for *vps23Δ*. TSG101-GFP was also identified in exosome samples consistent with results from fluorometry experiments (**Figure 6**).

The presence of 295 proteins in exosome samples from all strains studied raised the possibility that VPS23/TSG101 may not contribute to selection of most proteins sorted into exosomes. However, when I examined the relative abundance of these shared proteins that were identified in at least 2 of the 3 biological replicates conducted for each strain (i.e. proteins that were identified with confidence), I found that Hsc82, an Hsp90–type heat shock protein chaperone implicated in exosome–mediated thermotolerance (Oliver, 2021), was depleted from *vps23Δ* exosomes but was replenished when HsTSG101 was over–expressed (Figure 10C). Conversely, I found that Vps10, a carrier protein that shuttles newly synthesized proteins from the trans-Golgi network to endosome membranes, was enriched in *vps23Δ* exosomes but is normally depleted in wild type (**Figure 10D**) consistent with disrupted protein selection when VPS23 is deleted. Over-expression of HsTSG101 seemed to rescue this defect, as Vps10

was depleted like wild type in exosomes from *vps23Δ::TSG101-GFP* cells. All things considered, these preliminary results suggest that deleting VPS23 disrupts protein selection and sorting into exosomes, and HsTSG101 may in part rescue this defect.

3.6 HsTSG101 replaces ScVPS23 function in exosome-mediated thermotolerance

Given that ESCRT-I seems to be important for exosome protein selection, and Hsc82 – implicated in exosome-mediated thermotolerance (Oliver, 2021) – sorting into exosomes seems to be dependent on Vps23/TSG101, I next sought to determine if thermotolerance mediated by exosomes was affected by deleting ScVPS23 and replacing it with HsTSG101. I hypothesize that exosomes collected by ultracentrifugation from *vps23Δ* cells after thermotolerance conditioning (42°C for 30 minutes) will not confer thermotolerance to naïve yeast cells, as exosome protein selection and sorting of Hsc82 and other potentially bioactive proteins into exosome is likely defective. Exosomes collected from *vps23Δ::TSG101-GFP* cells should rescue this defect if HsTSG101 replaces ScVsp23 function. I tested this hypothesis by treating naïve (untreated) yeast cells with exosomes collected from separate yeast cultures and incubating them for 30 minutes at 30°C so they may respond to treatment. This was followed by challenging them with an extreme heat stress (50°C for 30 minutes), and then I stained them methylene blue to identify dead cells which were imaged by microscopy and counted to assess culture viability. The difference in viability observed with or without treatment (exosomes) was calculated to determine effects on thermotolerance.

I first measured thermotolerance conferred by conditioning alone by subjecting cultures to 42°C for 30 minutes without adding exosomes as a positive control and a standard to assess bioactivity conferred by exosome treatment (**Figure 11**). As previously reported (Oliver, 2021), I found that adding 0.1 μg of exosomes collected from wild type cells to naïve cultures (that were not conditioned) conferred thermotolerance, at levels similar to conditioning. Adding more wild type exosomes (0.25 μg) enhanced this effect demonstrating dose dependence (**Figure 11**). Next, I treated naïve yeast with exosomes collected from *vps23Δ* cells and found that they did not confer thermotolerance at low concentrations but could drive it when more were added (**Figure 11**), suggesting they are bioactive but efficacy is significantly reduced. I next treated naïve yeast with

exosomes collected from *vps23Δ::TSG101-GFP* cells and found that they conferred thermotolerance at levels similar to wild type exosomes (**Figure 11**). Given that HsTSG101 rescued the defect caused by ScVPS23 deletion, I conclude that HsTSG101 can replace ScVps23 function in exosome-mediated thermotolerance.

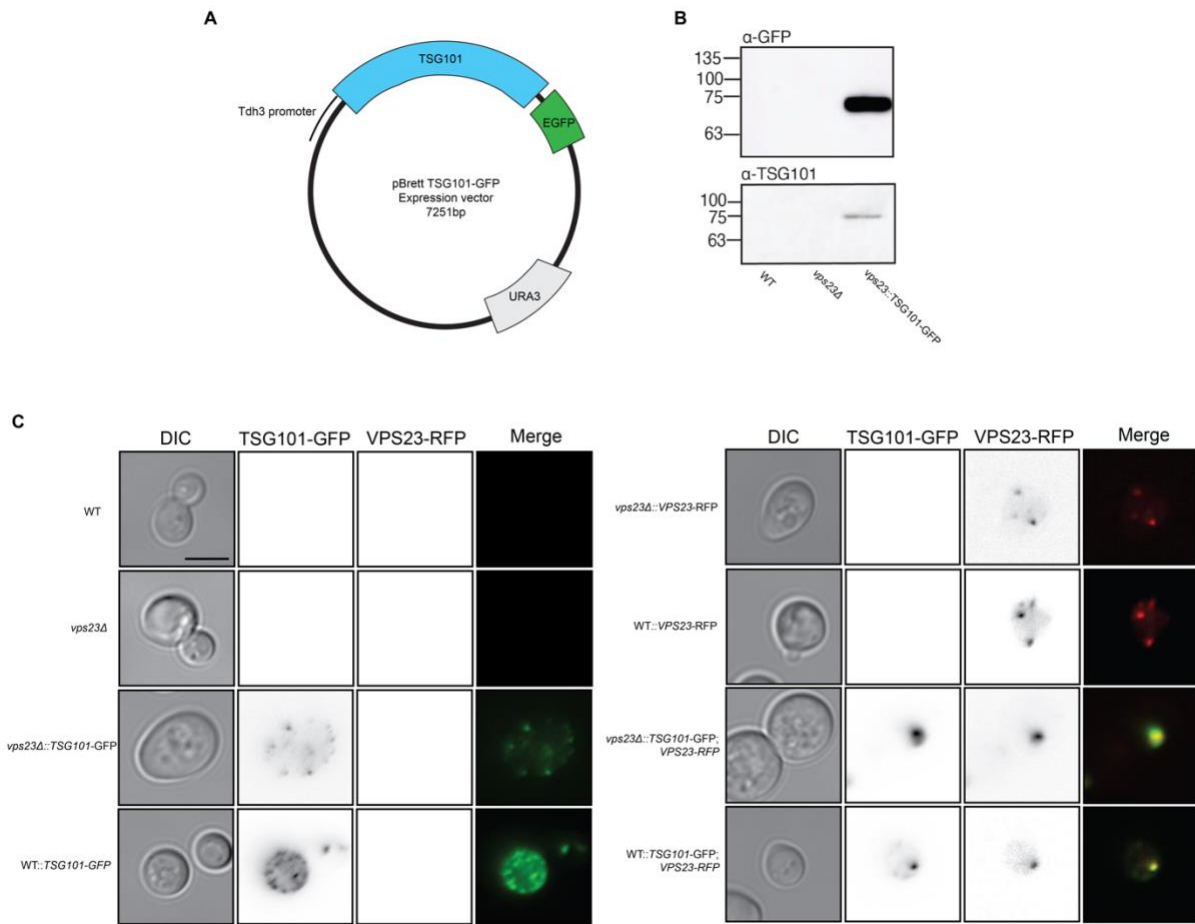


Figure 5. HsTSG101–GFP localizes to ScVPS23–positives sites when over-expressed in *S. cerevisiae*

(A) Map of plasmid encoding human TSG101 C-terminally tagged to GFP used in this study. **(B)** Western blots of whole cell lysates prepared from wild type (WT), *vps23Δ* and *vps23Δ::TSG101–GFP* cells using verified anti-GFP (top) or anti-TSG101 (bottom) antibodies. Expected molecular weight of TSG101–GFP is 70.9 kDa. Blots shown are representatives of 3 biological replicates (n = 3). **(C)** Fluorescence micrographs of live wild type (WT), *vps23Δ*, *vps23Δ::TSG101-GFP*, WT::TSG101-GFP, WT::VPS23-RFP, *vps23Δ::VPS23-RFP*, *vps23Δ::TSG101-GFP*; Vps23-RFP, and WT::TSG101-GFP; VPS23-RFP cells under control conditions (30°C). Merged GFP and RFP channels indicate colocalization (yellow). Micrographs shown represent experimental data from 3 biological replicates. Scale bar, 5 μm.

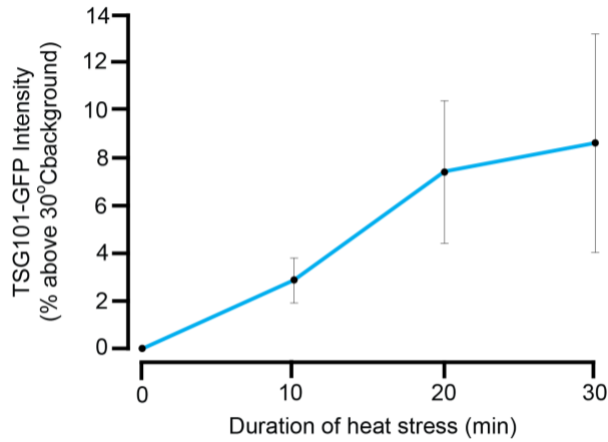


Figure 6. HsTSG101–GFP is released into the extracellular medium during heat stress

The extracellular medium was collected and filtered to enrich EVs from *yps23Δ::TSG101–GFP* cultures before (0) or 10, 20, 30 minute after heat stress (42°C). GFP fluorescence of samples was measured by fluorometry. Resulting values were background subtracted and normalized to values obtained before heat stress (t = 0 minutes). Error bars indicate S.E.M. (n = 3).

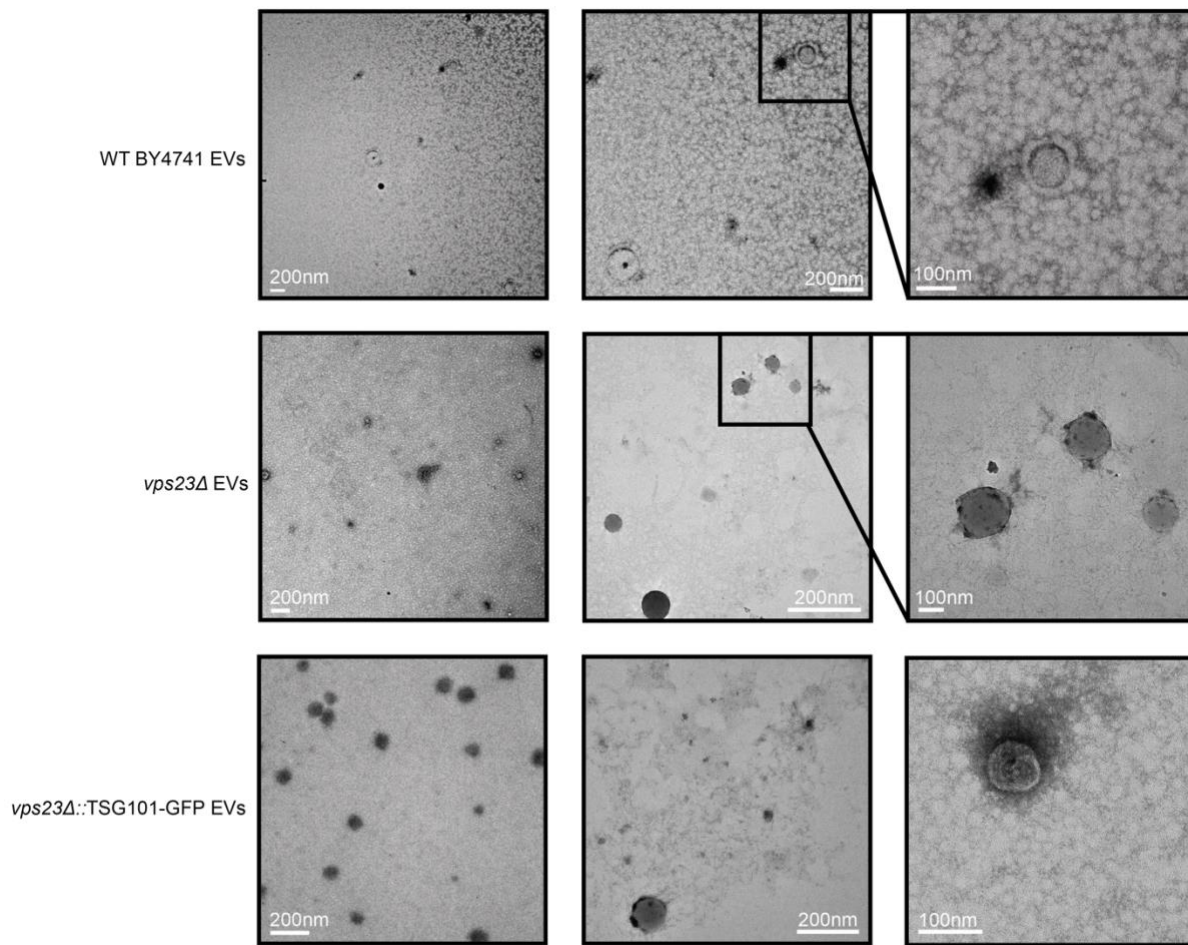


Figure 7. Transmission electron microscopy confirms exosomes are released with or without VPS23/TSG101

Transmission electron micrographs of EVs samples collected by filtration from wild type (WT), *vps23Δ*, or *vps23Δ::TSG101-GFP* yeast cells immediately after thermotolerance conditioning. Examples of relatively low magnification images are shown in the left and middle columns to demonstrate that particles (EVs) are abundant; Scale bars, 200 nm. Higher magnification images are shown in the right column to demonstrate that particles (EVs) are membrane-bound; Scale bars, 100 nm.

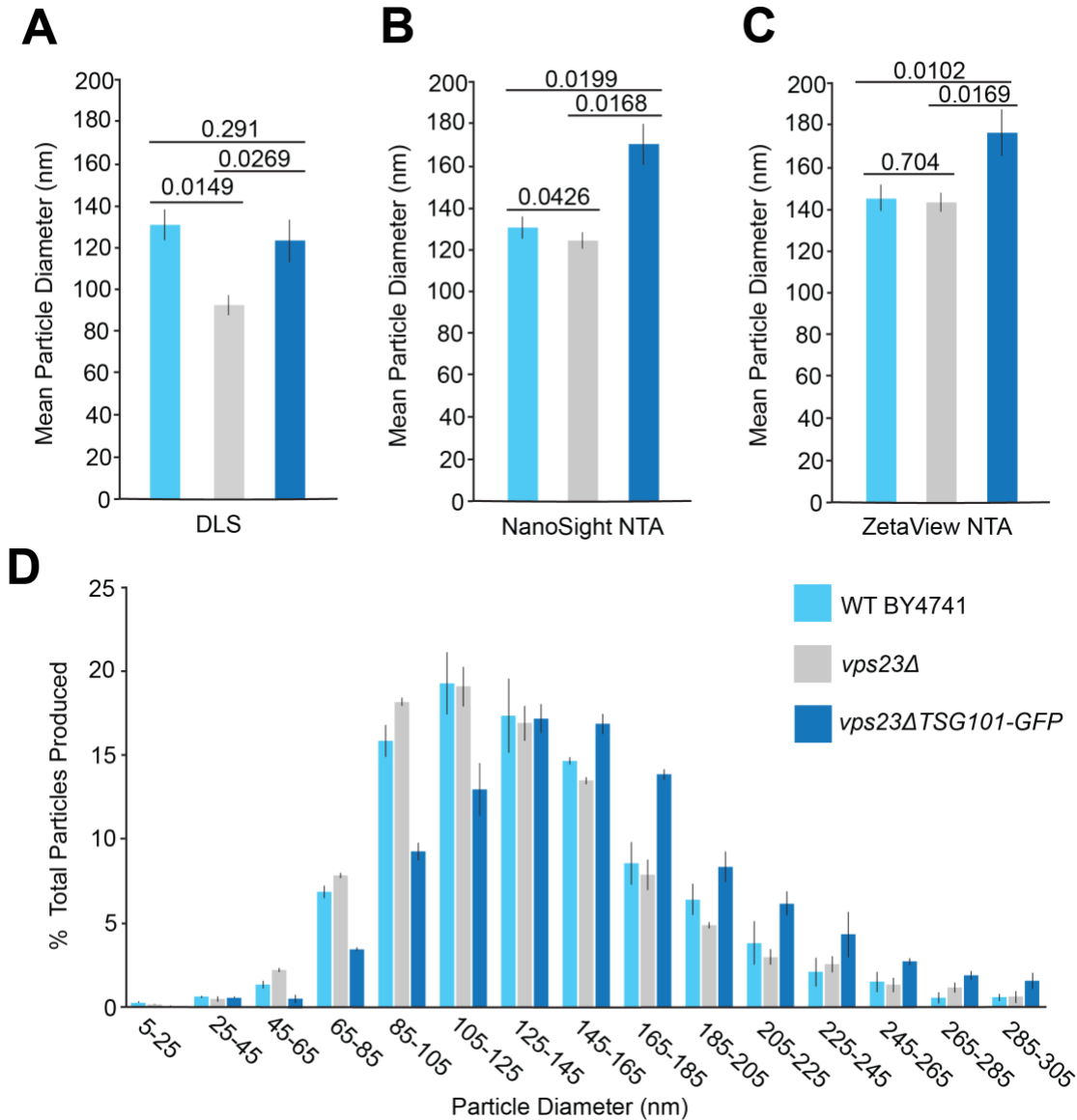


Figure 8. EV size measurements using 3 methods confirms that ESCRT-I is not involved in exosome formation or release

(A – C) Mean particle sizes of EV samples collected by filtration immediately after heat stress (42°C for 30 minutes) from wild type (WT), *vps23Δ* or *vps23Δ::TSG101-GFP* yeast cells measured using dynamic light scattering (A) NanoSight NTA (B) or ZetaView NTA (C). Mean values ± S.E.M. are shown. P-values from Student’s 2-tailed t-tests are shown for comparisons; P-values ≤ 0.05 indicate significant differences. (D) Distributions of particle (EV) populations collected from each strain based on diameter determined by ZetaView NTA. Error bars indicate S.E.M. (n = 3).

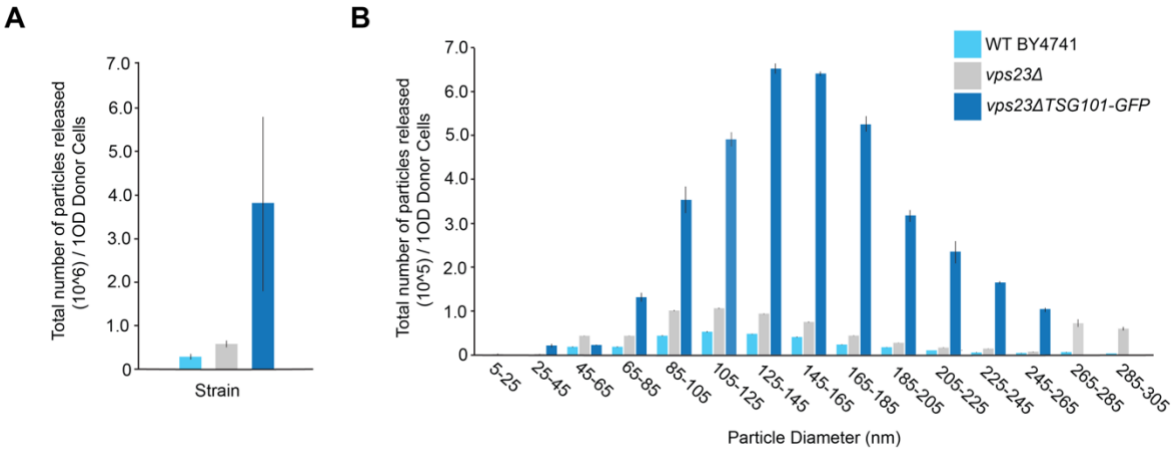


Figure 9. HsTSG101–GFP over–expression increases exosome numbers

Total number of particles (A) and size distribution of these particles (B) collected by filtration from 3×10^7 (1 OD_{600nm} unit of) wild type, *vps23Δ*, or *vps23Δ::TSG101-GFP* cells after thermotolerance conditioning measured using ZetaView NTA. Mean values ± S.E.M. are shown (n = 3).

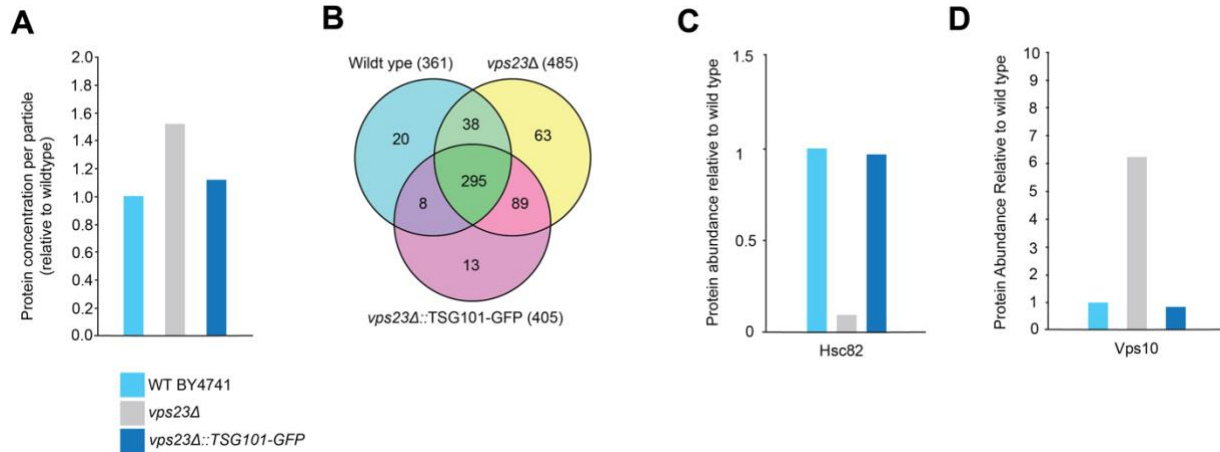


Figure 10. Vps23/TSG101 regulates yeast exosome protein content

(A) Total protein content of exosomes collected by ultracentrifugation from wild type, *vps23Δ* or *vps23Δ::TSG101-GFP* cells after thermotolerance conditioning measured by Bradford assay. Particle number measurements by ZetaView NTA were used to calculate amount of protein per particle (exosome). Mean values shown (n = 3). (B) Venn diagram indicating shared or unique proteins identified in exosomes collected by ultracentrifugation from wild type, *vps23Δ*, and *vps23Δ::TSG101-GFP* after heat stress. Proteomic datasets from 3 biological replicates were pooled for each strain and all proteins identified are shown. (C, D) Exosome protein abundance relative to wild type levels of the Hsp90 ortholog Hsc82 (C) or the sorting receptor Vps10 (D) for samples prepared from wild type, *vps23Δ* or *vps23Δ::TSG101-GFP* cells. These proteins were present in at least 2 of 3 biological replicates for each strain and mean abundance based on peptide counts and coverage was estimated by mass spectrometry.

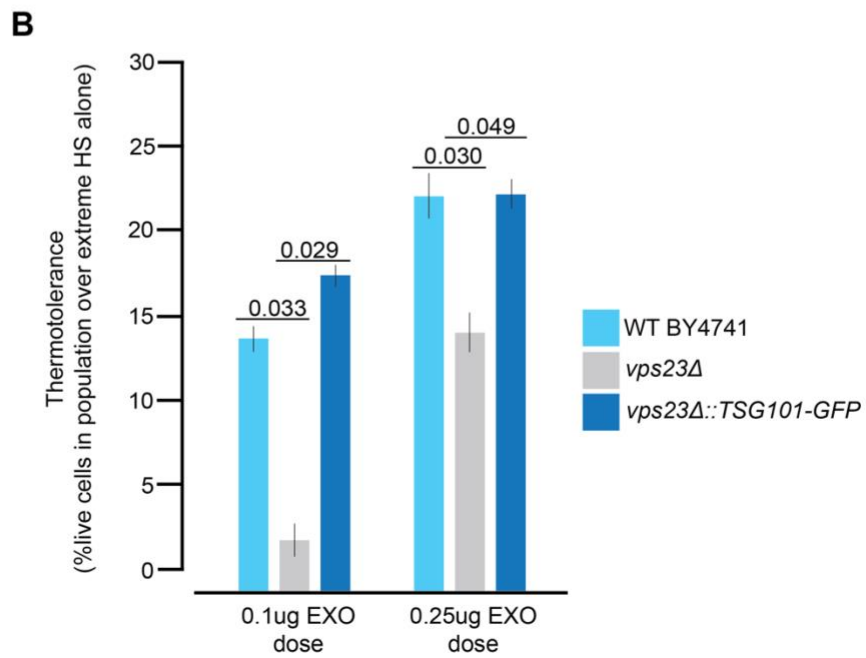
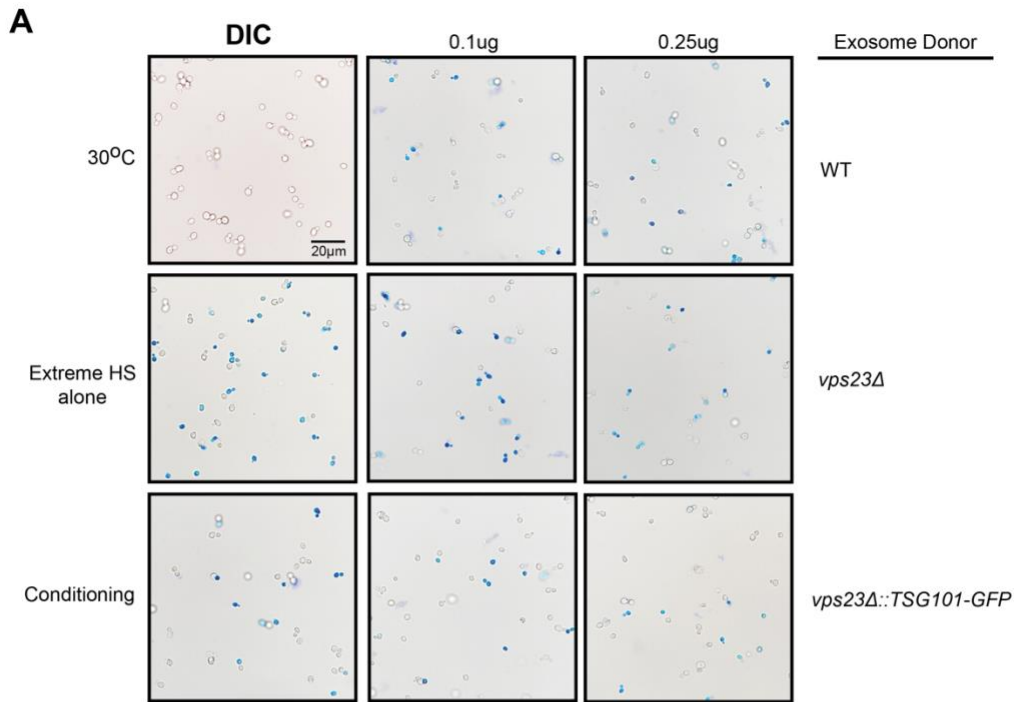


Figure 11. HsTSG101 rescues defects in exosome-mediated thermotolerance caused by ScVPS23 deletion

(A) Examples of light micrographs used to calculate thermotolerance. Cells were stained with methylene blue to detect dead yeast cells. Cultures of *vps23Δ* cells were examined prior to treatment at 30°C (Control), after extreme heat stress (50°C for 30 minutes; Extreme HS alone) or after thermotolerance conditioning followed by extreme heat stress (Conditioning). In place of conditioning, naïve cells were treated with 0.1 or 0.25 μg of exosomes collected from separate wild type, *vps23Δ* or *vps23Δ::TSG101-GFP* cultures. Scale bar, 20 μm. (B) Thermotolerance was measured for conditioning or exosomes treatments shown in (A) by calculating the difference between viability observed with or without treatments prior to application of extreme heat stress. Mean ± S.E.M. are shown representing data from three biological replicates. Comparisons shown were assessed using Student's 2-tailed t-tests and resulting P-values are shown. $P \leq 0.05$ is considered significant.

CHAPTER 4 – DISCUSSION

4.1 HsTSG101 seems to replace ScVPS23 function in exosome-mediated thermotolerance

Herein, I tested the hypothesis that human TSG101, when ectopically expressed, may functional replace endogenous VPS23, a component of ESCRT-I critical for protein selection, in exosome-mediated thermotolerance in *S. cerevisiae*. I find that TSG101, tagged to GFP and when over-expressed, seems to localize to the same sites as native ScVps23 within live cells where exosome biogenesis occurs (**Figure 6**). Here it likely gets sorted into exosomes, as I observe TSG101-GFP expression in the extracellular medium after cells are exposed to heat conditioning (**Figure 7**), and it is identified in purified exosome fractions by mass spectrometry. As expected (because VPS23/TSG101 does not impact vesicle membrane formation), I confirmed that exosome morphology was not impacted by swapping ScVPS23 with human TSG101 (**Figure 8**) and exosome size was not significantly affected when measured using three different methods (**Figure 9**). However, over-expressing TSG101 seemed to increase the number of exosomes released (**Figure 11**). Deleting VPS23 altered protein content of exosomes, including loss of a specific protein implicated in thermotolerance, but replacing it with HsTSG101 partially rescued protein abundance and selection (**Figure 12**). In support, exosomes isolated from *vps23* Δ cells showed defects in conferring thermotolerance, whereas replacing it with HsTSG101 rescued this effect (**Figure 13**). All things considered, I conclude that HsTSG101 seems to, at least in part, replace ScVPS23 function in protein sorting into exosomes important for thermotolerance.

4.2 ScVps23 contributes to exosome protein selection and sorting for bioactivity

Prior to this study, it was clear that all eukaryotic cells studied employ ESCRTs for selective protein degradation by the MVB pathway, and other cellular processes, but their contributions to exosome biology are understudied. Herein, I found that the ESCRT-I component Vps23 seems to play a role in exosome protein selection and loading (**Figure 10**) necessary for conferring thermotolerance in *S. cerevisiae* (**Figure 11**). This is compatible with its known role in selecting and loading proteins into ILVs for degradation (Babst et al., 2000; Katzmann et al., 2002). A similar observation was made in a previous report – one of few on *S. cerevisiae* EV biology –

whereby it was shown that deleting *vps23Δ* changed protein content of EVs released from *S. cerevisiae* when unstressed (Zhao et al., 2019). Specifically, proteins involved with cell wall biosynthesis including Fks1, Chs1 and Chs3 seemed to be more enriched in *vps23Δ* EVs than wild type. In support, when these *vps23Δ* EVs were added to yeast cultures, they seemed to improve cell survival after imposing cell wall stress with the drug caspofungin, i.e. the knock mutation led to a gain-of-function phenotype. Herein, I exclusively isolated EVs after thermotolerance conditioning (not during culture growth when cells are untreated) and thus did not attempt to replicate these results. But both findings support the idea that Vps23 contributes to EV protein selection and sorting required for their bioactivity.

However, my findings were not entirely consistent with other observations made in this report (Zhao et al., 2019): First, using mass spectrometry, they identified 3,133 proteins in EV samples prepared from wild type cells, representing 52% of the *S. cerevisiae* proteome. I identified 361 proteins in exosomes collected from wild type cells, representing only 6% of the proteome (**Figure 10B**). Noting that because over half of the proteome was identified in their study, I could not justify comparing our datasets to demonstrate consistency or to validate my findings. Regardless, only my results are consistent with a protein selection and sorting mechanism (e.g. ESCRT-I) being in place to restrict protein entry into exosomes. Second, although supporting data is limited, they claim that *vps23Δ* release fewer EVs. I did not replicate these findings and find that deleting *VPS23* may, if anything, slightly increase exosome release (**Figure 9**). Again, only my results support the canonical model of ESCRT-mediated ILV/exosome biosynthesis.

Lastly, although small EVs continue to be released from *vps23Δ* cells, consistent with my results, they observed an increase in release of larger EVs (150 – 500 nm diameter; Zhao et al., 2019). I did not make the same observation as deleting *vps23Δ* seemed to have no effect on EV size when using NTA, the same method of measurement (**Figure 8**). Again, my results are more consistent with the existing literature and canonical model of ESCRT function, whereby ESCRT-I does not contribute to vesicle formation (i.e. membrane deformation and cleavage) and thus should not severely alter vesicle size, e.g. increase it from 100 nm to 500 nm as reported by Zhao and colleagues (Zhao et al., 2019). Moreover, this size is in the range of microvesicles or

ectosomes, a different EV class than exosomes, which are synthesized by outward projection from the plasma membrane (They et al., 2009). Although the porous yeast cell wall can accommodate release of small vesicles from intracellular stores (i.e. exosomes), it is unlikely that it supports outward budding and cleavage, as well as passage, of larger EVs up to 500 nm in diameter. Further, orthologous machinery thought underlie microvesicle biosynthesis has not confirmed to be present in yeasts.

One possible explanation for these potential discrepancies is I collected a relatively homogeneous population of EVs (exosomes) only during a narrow, experimentally-defined window (42°C for 30 minutes) under mild heat stress which is known to induce EV-sharing in many organisms (REFs from intro). Whereas Zhao and colleagues collected a heterogeneous population of EVs that were constitutively released from yeast cultures grown for 19 – 24 hours, i.e. the physiological context of EV biogenesis and release is unclear and EVs present in samples were released during very different phases of culture growth. Despite this, results from both studies implicate VSP23 in EV protein selection and sorting needed for their bioactivity.

4.3 Vps23/TSG101 function in exosome biology seems deeply conserved

The primary goal of this study was to determine whether human TSG101 may replace Vps23 function in *S. cerevisiae* to better understand the basis of fundamental exosome biogenesis and cargo selection. I found that, when over-expressed and tagged to GFP, HsTSG101 localized to the same intracellular sites as ScVps23 (**Figure 5B**), suggesting that the signal for proper protein trafficking was conserved. In support, HsTSG101-GFP was detected within exosomes released during thermotolerance conditioning by fluorometry (**Figure 6**) and proteomics analysis by mass spectrometry (data not shown). This suggested that it was packaged into exosomes, presumably at endosomes resembling puncta within cells, as is observed in mammalian exosomes (**Figure 5**) (Bishop et al., 2001; Tucher et al., 2018). Although I did not test the idea, this result raises the possibility that HsTSG101 may assemble into the ESCRT-I protein complex with other yeast protein subunits, a requisite for ESCRT-I function, at endosome membranes (Katzmann et al., 2001). In support, when ScVPS23 is replaced with HsTSG101, I find that it partially rescues exosome protein selection and sorting (**Figure 10**), the primary function of ESCRT-I. This

included rescuing the proper exosomal selection and sorting of Hsc82, a heat shock protein chaperone critical for exosome-mediated thermotolerance in yeast (**Figure 10C**) (Oliver, 2021). This observation correlates with loss of thermotolerance conferred by exosomes when VPS23 was deleted and complete rescue when HsTSG101 replaced it (**Figure 11**). Further investigation is necessary to validate these results, e.g. immunogold labeling and TEM of exosomes to demonstrate TSG101 is contained within them, confirmation that Hsc82 binds Vps23/TSG101 and is contributing the effects on exosome-mediated thermotolerance, and demonstrating that TSG101 binds ScVps28 and ScVps37 to form an intact ESCRT-I. However, from the data presented, it seems that HsTSG101 can, at least in part, replace ScVSP23 function in selecting and sorting proteins like Hsc82 into exosomes that is critical for conferring thermotolerance in *S. cerevisiae*, revealing that the role of ESCRT-I in exosome biogenesis is deeply conserved amongst eukaryotes.

Prior to this study, others had published a short report claiming that HsTSG101 cannot replace Vps23 function in context to its conventional role in selecting transporter and receptor proteins for degradation by the MVB pathway (Blanco & Lazo., 2003). However, despite being difficult to read and comprehend, the report presents only two datasets to support this conclusion that assessed yeast culture growth or alpha-factor secretion, and phenotypes were unclear given the lack of controls. Importantly, they did not measure transporter or receptor protein degradation (a glaring omission) and HsTSG101 seemed to abnormally localize to the nucleus based on the (poor quality) micrographs presented. Thus, their conclusion is invalid and given my new findings, it seems warranted to properly test the hypothesis that HsTSG101 can also replace ScVPS23 function in the MVB pathway.

Also prior to this study, it was unclear if ScVps23 can select and sort soluble, cytoplasmic proteins into ILVs at endosome membranes, as only its role(s) in transmembrane protein (transporter, receptor) degradation have been characterized (Babst et al., 2000; Katzmann et al., 2002). Although very preliminary, I find that deleting VSP23 decreases sorting of soluble proteins like Hsc82 into ILV/exosomes by proteomics analysis (**Figure 10**). HsTSG101, on the other hand, is implicated in soluble protein selection and sorting, including cargoes like heat shock proteins (Giordano et al., 2019), consistent with my findings. This is particularly critical

for exosome function, as soluble proteins like heat shock proteins must be selected and packaged within their lumen to confer bioactivity. Thus, I speculate that ScVps23 like HsTSG101 may recognize both classes of cargo proteins, a hypothesis warranting further study.

In mammalian cells, both over-expression of TSG101 and knock-down of TSG101 were shown to reduce secretion of EVs (Boker et al., 2018); conflicting results that offer little interpretation of the underlying mechanism. However, herein I find that expression of HsTSG101-GFP behind a strong promoter (TDH3) on a high-copy number (2 μ) plasmid (likely constituting over-expression) in *S. cerevisiae* lacking VPS23 results in a large (14-fold) increase in exosome release compared to wild type (**Figure 9**). Notably, these exosomes seem to contain a normal amount of protein (**Figure 10A**) and content is similar to wild type (**Figure 10B – D**), suggesting that protein selection and sorting is intact. However, I find that these EVs are slightly larger than those from WT cells based on NTA (**Figure 8B – D**), noting that the size of nearly all EVs released are still in the range of exosomes (30 – 200 nm). This latter result brings up the possibility that HsTSG101 may regulate other aspects of exosome biogenesis, aside from protein selection and sorting. Whether this is an artifact of over-expression or is a property of the HsTSG101 protein is unclear. But this can be resolved in the future by further characterizing yeast strains over-expressing ScVps23-RFP shown in **Figure 5B**, whereby if they are found to also secrete larger exosomes then this function is conserved across species. Alternatively, this could be resolved by placing HsTSG101 behind the native promoter of ScVPS23 (instead of TDH3) or integrating it into the genome in place of VSP23 to eliminate effects of over-expression. Regardless, this observation is intriguing from a exosome bioproduction perspective, as this *vsp23 Δ ::TSG101-GFP* strain could be used to generate high amounts of purified exosomes for future studies.

4.4 Conclusion and future directions

In all, I conclude that Vps23/TSG101 plays a deeply conserved function in ESCRT-mediated exosome biogenesis, whereby these orthologs seem to share the ability to select and sort proteins into exosomes presumably using a common mechanism conserved from yeast to human. This function is particularly important for mediating physiological responses to (heat) stress, a

fundamental property of exosomes observed in humans and all eukaryotic organisms studied. Future studies will focus on better resolving the mechanism of cargo protein recognition, which will involve determining if HsTSG101 prefers to select and sort human cargo proteins, over yeast ones, into exosomes. Also, expanding these studies to include assessment of ScBro1/HsALIX orthology would provide a more comprehensive understanding of exosome protein selection and loading, and may reveal different roles in fundamental EV biology.

References

- Akers JC, Gonda D, Kim R, Carter BS, Chen CC. Biogenesis of extracellular vesicles (EV): exosomes, microvesicles, retrovirus-like vesicles, and apoptotic bodies. *J Neurooncol*. 2013 May;113(1):1-11. doi: 10.1007/s11060-013-1084-8.
- Babst M, Odorizzi G, Estepa EJ, Emr SD. Mammalian tumor susceptibility gene 101 (TSG101) and the yeast homologue, Vps23p, both function in late endosomal trafficking. *Traffic*. 2000 Mar;1(3):248-58. doi: 10.1034/j.1600-0854.2000.010307.x.
- Bagnat M, Keränen S, Shevchenko A, Shevchenko A, Simons K. Lipid rafts function in biosynthetic delivery of proteins to the cell surface in yeast. *Proc Natl Acad Sci U S A*. 2000 Mar 28;97(7):3254-9. doi: 10.1073/pnas.97.7.3254.
- Baietti MF, Zhang Z, Mortier E, Melchior A, Degeest G, Geeraerts A, Ivarsson Y, Depoortere F, Coomans C, Vermeiren E, Zimmermann P, David G. 2012. Syndecan-syntenin-ALIX regulates the biogenesis of exosomes. *Nat Cell Biol*.3;14(7):677-85. doi: 10.1038/ncb2502.
- Bari, R., Guo, Q., Xia, V., Zhang, YH., Giesert, EE., Levy, S, et al. (2011) Tetraspanins regulate the protrusive activities of cell membrane. *Biochem Biophys Res Commun*. 415(4):619-26. doi:10.1016/j.bbrc.2011.10.121
- Battistelli M, Falcieri E. 2020. Apoptotic Bodies: Particular Extracellular Vesicles Involved in Intercellular Communication. *Biology (Basel)*. 20;9(1):21. doi: 10.3390/biology9010021
- Beit-Yannai E, Tabak S, Stamer WD. Physical exosome:exosome interactions. *J Cell Mol Med*. 2018 Mar;22(3):2001-2006. doi: 10.1111/jcmm.13479.
- Bellingham SA, Guo BB, Coleman BM, Hill AF. Exosomes: vehicles for the transfer of toxic proteins associated with neurodegenerative diseases? *Front Physiol*. 2012 May 3;3:124. doi: 10.3389/fphys.2012.00124.
- Bishop N, Woodman P. TSG101/mammalian VPS23 and mammalian VPS28 interact directly and are recruited to VPS4-induced endosomes. *J Biol Chem*. 2001 Apr 13;276(15):11735-42. doi: 10.1074/jbc.M009863200.
- Bishop N, Horman A, Woodman P. Mammalian class E vps proteins recognize ubiquitin and act in the removal of endosomal protein-ubiquitin conjugates. *J Cell Biol*. 2002 Apr 1;157(1):91-101. doi: 10.1083/jcb.200112080.
- Blanco S, Lazo PA. 2003. Human TSG101 does not replace *Saccharomyces cerevisiae* VPS23 role in the quality control of plasma membrane proteins. *FEMS Microbiol Lett*. 25;221(2):151-4. doi: 10.1016/S0378-1097(03)00179-4.

Böker KO, Lemus-Diaz N, Rinaldi Ferreira R, Schiller L, Schneider S, Gruber J. 2018. The Impact of the CD9 Tetraspanin on Lentivirus Infectivity and Exosome Secretion. *Mol Ther.* Feb 7;26(2):634-647. doi: 10.1016/j.ymthe.2017.11.008.

Borges F., Reis L., Schor N. 2013. Extracellular vesicles: Structure, function, and potential clinical uses in renal diseases. *Braz. J. Med. Biol. Res.* 46:824–830. doi: 10.1590/1414-431X20132964.

Bose S, Aggarwal S, Singh DV, Acharya N. 2020. Extracellular vesicles: An emerging platform in gram-positive bacteria. *Microb Cell.*5;7(12):312-322. doi: 10.15698/mic2020.12.737.

Brinton LT, Sloane HS, Kester M, Kelly KA. Formation and role of exosomes in cancer. *Cell Mol Life Sci.* 2015 Feb;72(4):659-71. doi: 10.1007/s00018-014-1764-3

Cai J, Wu J, Wang J, Li Y, Hu X, Luo S, Xiang D. Extracellular vesicles derived from different sources of mesenchymal stem cells: therapeutic effects and translational potential. *Cell Biosci.* 2020 May 24;10:69. doi: 10.1186/s13578-020-00427-x.

Buschow SI, Liefhebber JM, Wubbolts R, Stoorvogel W. Exosomes contain ubiquitinated proteins. *Blood Cells Mol Dis.* 2005 Nov-Dec;35(3):398-403. doi: 10.1016/j.bcmd.2005.08.005.

Caruso S, Atkin-Smith GK, Baxter AA, Tixeira R, Jiang L, Ozkocak DC, Santavanond JP, Hulett MD, Lock P, Phan TK, Poon IKH. Defining the role of cytoskeletal components in the formation of apoptopodia and apoptotic bodies during apoptosis. *Apoptosis.* 2019 Dec;24(11-12):862-877. doi: 10.1007/s10495-019-01565-5.

Caruso S, Poon IKH. Apoptotic Cell-Derived Extracellular Vesicles: More Than Just Debris. *Front Immunol.* 2018 Jun 28;9:1486. doi: 10.3389/fimmu.2018.01486.

Chronopoulos A, Kalluri R. Emerging role of bacterial extracellular vesicles in cancer. *Oncogene.* 2020 Nov;39(46):6951-6960. doi: 10.1038/s41388-020-01509-3.

Chu T, Sun J, Saksena S, Emr SD. New component of ESCRT-I regulates endosomal sorting complex assembly. *J Cell Biol.* 2006 Dec 4;175(5):815-23. doi: 10.1083/jcb.200608053.

Chua HH, Lee HH, Chang SS, Lu CC, Yeh TH, Hsu TY, Cheng TH, Cheng JT, Chen MR, Tsai CH. 2006. Role of the TSG101 gene in Epstein-Barr virus late gene transcription. *J Virol.* 2007 Mar;81(5):2459-71. doi: 10.1128/JVI.02289-06.

Colombo M, Moita C, van Niel G, Kowal J, Vigneron J, Benaroch P, Manel N, Moita LF, Théry C, Raposo G. 2013. Analysis of ESCRT functions in exosome biogenesis, composition and secretion highlights the heterogeneity of extracellular vesicles. *J Cell Sci.* 2013 Dec 15;126(Pt 24):5553-65. doi: 10.1242/jcs.128868

Conde-Vancells J, Rodriguez-Suarez E, Embade N, Gil D, Matthiesen R, Valle M, Elortza F, Lu SC, Mato JM, Falcon-Perez JM. Characterization and comprehensive proteome profiling of

exosomes secreted by hepatocytes. *J Proteome Res.* 2008 Dec;7(12):5157-66. doi: 10.1021/pr8004887.

Curtiss M, Jones C, Babst M. Efficient cargo sorting by ESCRT-I and the subsequent release of ESCRT-I from multivesicular bodies requires the subunit Mvb12. *Mol Biol Cell.* 2007 Feb;18(2):636-45. doi:10.1091/mbc.e06-07-0588.

Dawaliby R, Trubbia C, Delporte C, Noyon C, Ruyschaert JM, Van Antwerpen P, Govaerts C. Phosphatidylethanolamine Is a Key Regulator of Membrane Fluidity in Eukaryotic Cells. *J Biol Chem.* 2016 Feb 12;291(7):3658-67. doi: 10.1074/jbc.M115.706523.

Dawson CS, Garcia-Ceron D, Rajapaksha H, Faou P, Bleackley MR, Anderson MA. Protein markers for *Candida albicans* EVs include claudin-like Sur7 family proteins. *J Extracell Vesicles.* 2020 Apr 16;9(1):1750810. doi: 10.1080/20013078.2020.1750810

Dolnik O, Kolesnikova L, Welsch S, Strecker T, Schudt G, Becker S. 2014. Interaction with Tsg101 is necessary for the efficient transport and release of nucleocapsids in marburg virus-infected cells. *PLoS Pathog.* 2014 Oct 16;10(10):e1004463. doi: 10.1371/journal.ppat.1004463.

Donoso-Quezada J, Ayala-Mar S, González-Valdez J. The role of lipids in exosome biology and intercellular communication: Function, analytics and applications. *Traffic.* 2021 Jul;22(7):204-220. doi: 10.1111/tra.12803.

Dou G, Tian R, Liu X, Yuan P, Ye Q, Liu J, Liu S, Zhou J, Deng Z, Chen X, Liu S, Jin Y. Chimeric apoptotic bodies functionalized with natural membrane and modular delivery system for inflammation modulation. *Sci Adv.* 2020 Jul 22;6(30):eaba2987. doi:10.1126/sciadv.aba2987.

Doyle LM, Wang MZ. 2019. Overview of Extracellular Vesicles, Their Origin, Composition, Purpose, and Methods for Exosome Isolation and Analysis. *Cells.* 2019 Jul 15;8(7):727. doi: 10.3390/cells8070727.

Edgar JR. Q&A: What are exosomes, exactly? *BMC Biol.* 2016 Jun 13;14:46. doi: 10.1186/s12915-016-0268-z.

Eldh M, Ekström K, Valadi H, Sjöstrand M, Olsson B, Jernås M, Lötvall J. Exosomes communicate protective messages during oxidative stress; possible role of exosomal shuttle RNA. *PLoS One.* 2010 Dec 17;5(12):e15353. doi: 10.1371/journal.pone.0015353.

Elsherbini A, Qin H, Zhu Z, Tripathi P, Wang G, Crivelli SM, Spassieva SD, Bieberich E. Extracellular Vesicles Containing Ceramide-Rich Platforms: "Mobile Raft" Isolation and Analysis. *Methods Mol Biol.* 2021;2187:87-98. doi: 10.1007/978-1-0716-0814-2_5.

Galao RP, Scheller N, Alves-Rodrigues I, Breinig T, Meyerhans A, Díez J. *Saccharomyces cerevisiae*: a versatile eukaryotic system in virology. *Microb Cell Fact.* 2007 Oct 10;6:32. doi: 10.1186/1475-2859-6-32.

Galleu A, Riffo-Vasquez Y, Trento C, Lomas C, Dolcetti L, Cheung TS, von Bonin M, Barbieri L, Halai K, Ward S, Weng L, Chakraverty R, Lombardi G, Watt FM, Orchard K, Marks DI, Apperley J, Bornhauser M, Walczak H, Bennett C, Dazzi F. Apoptosis in mesenchymal stromal cells induces in vivo recipient-mediated immunomodulation. *Sci Transl Med*. 2017 Nov 15;9(416):eaam7828. doi: 10.1126/scitranslmed.aam7828

Garrus JE, von Schwedler UK, Pornillos OW, Morham SG, Zavitz KH, Wang HE, Wettstein DA, Stray KM, Côté M, Rich RL, Myszka DG, Sundquist WI. 2001.Tsg101 and the vacuolar protein sorting pathway are essential for HIV-1 budding. *Cell*. 5;107(1):55-65. doi: 10.1016/s0092-8674(01)00506-2.

Gebara, N., Rossi, A., Skovronova, R. *et al.* 2020. Extracellular Vesicles, Apoptotic Bodies and Mitochondria: Stem Cell Bioproducts for Organ Regeneration. *Curr Transpl Rep* 7, 105–113. doi.org/10.1007/s40472-020-00282-2

Gebremedhn S, Gad A, Aglan HS, Laurincik J, Prochazka R, Salilew-Wondim D, Hoelker M, Schellander K, Tesfaye D. Extracellular vesicles shuttle protective messages against heat stress in bovine granulosa cells. *Sci Rep*. 2020 Sep 25;10(1):15824. doi: 10.1038/s41598-020-72706-z.

Gill DJ, Teo H, Sun J, Perisic O, Veprintsev DB, Emr SD, Williams RL. Structural insight into the ESCRT-I/II link and its role in MVB trafficking. *EMBO J*. 2007 Jan 24;26(2):600-12. doi: 10.1038/sj.emboj.7601501.

Gill S, Catchpole R, Forterre P. Extracellular membrane vesicles in the three domains of life and beyond. *FEMS Microbiol Rev*. 2019 May 1;43(3):273-303. doi: 10.1093/femsre/fuy042.

Giordano C, Gelsomino L, Barone I, Panza S, Augimeri G, Bonofiglio D, Rovito D, Naimo GD, Leggio A, Catalano S, Andò S. Leptin Modulates Exosome Biogenesis in Breast Cancer Cells: An Additional Mechanism in Cell-to-Cell Communication. *J Clin Med*. 2019 Jul 12;8(7):1027. doi: 10.3390/jcm8071027.

Guan XL, Souza CM, Pichler H, Dewhurst G, Schaad O, Kajiwara K, Wakabayashi H, Ivanova T, Castillon GA, Piccolis M, Abe F, Loewith R, Funato K, Wenk MR, Riezman H. Functional interactions between sphingolipids and sterols in biological membranes regulating cell physiology. *Mol Biol Cell*. 2009 Apr;20(7):2083-95. doi: 10.1091/mbc.e08-11-1126.

Gutiérrez-Vázquez C, Villarroya-Beltri C, Mittelbrunn M, Sánchez-Madrid F. Transfer of extracellular vesicles during immune cell-cell interactions. *Immunol Rev*. 2013 Jan;251(1):125-42. doi: 10.1111/imr.12013.

Grant BD, Donaldson JG. Pathways and mechanisms of endocytic recycling. *Nat Rev Mol Cell Biol*. 2009;10:597–608. doi: 10.1038/nrm2755.

Han QF, Li WJ, Hu KS, Gao J, Zhai WL, Yang JH, Zhang SJ. Exosome biogenesis: machinery, regulation, and therapeutic implications in cancer. *Mol Cancer*. 2022 Nov 1;21(1):207. doi: 10.1186/s12943-022-01671-0.

Hanson PI, Cashikar A. Multivesicular body morphogenesis. *Annu Rev Cell Dev Biol*. 2012;28:337-62. doi: 10.1146/annurev-cellbio-092910-154152.

Hauser P, Wang S, Didenko VV. Apoptotic Bodies: Selective Detection in Extracellular Vesicles. *Methods Mol Biol*. 2017;1554:193-200. doi: 10.1007/978-1-4939-6759-9_12.

Heijnen HF, Schiel AE, Fijnheer R, Geuze HJ, Sixma JJ. Activated platelets release two types of membrane vesicles: microvesicles by surface shedding and exosomes derived from exocytosis of multivesicular bodies and alpha-granules. *Blood*. 1999 Dec 1;94(11):3791-9.

Henne WM, Stenmark H, Emr SD. Molecular mechanisms of the membrane sculpting ESCRT pathway. *Cold Spring Harb Perspect Biol*. 2013 Sep 1;5(9):a016766. doi:10.1101/cshperspect.a016766.

Horbay R, Hamraghani A, Ermini L, Holcik S, Beug ST, Yeganeh B. Role of Ceramides and Lysosomes in Extracellular Vesicle Biogenesis, Cargo Sorting and Release. *Int J Mol Sci*. 2022 Dec 5;23(23):15317. doi: 10.3390/ijms232315317.

Hoshino A, Kim HS, Bojmar L, Gyan KE, Cioffi M, Hernandez J, Zambirinis CP, Rodrigues G, Molina H, Heissel S, Mark MT, Steiner L, Benito-Martin A, Lucotti S, Di Giannatale A, Offer K, Nakajima M, Williams C, Nogués L, Pelissier Vatter FA, Hashimoto A, Davies AE, Freitas D, Kenific CM, Ararso Y, Buehring W, Lauritzen P, Ogitani Y, Sugiura K, Takahashi N, Alečković M, Bailey KA, Jolissant JS, Wang H, Harris A, Schaeffer LM, García-Santos G, Posner Z, Balachandran VP, Khakoo Y, Raju GP, Scherz A, Sagi I, Scherz-Shouval R, Yarden Y, Oren M, Malladi M, Petriccione M, De Braganca KC, Donzelli M, Fischer C, Vitolo S, Wright GP, Ganshaw L, Marrano M, Ahmed A, DeStefano J, Danzer E, Roehrl MHA, Lacayo NJ, Vincent TC, Weiser MR, Brady MS, Meyers PA, Wexler LH, Ambati SR, Chou AJ, Slotkin EK, Modak S, Roberts SS, Basu EM, Diolaiti D, Krantz BA, Cardoso F, Simpson AL, Berger M, Rudin CM, Simeone DM, Jain M, Ghajar CM, Batra SK, Stanger BZ, Bui J, Brown KA, Rajasekhar VK, Healey JH, de Sousa M, Kramer K, Sheth S, Baisch J, Pascual V, Heaton TE, La Quaglia MP, Pisapia DJ, Schwartz R, Zhang H, Liu Y, Shukla A, Blavier L, DeClerck YA, LaBarge M, Bissell MJ, Caffrey TC, Grandgenett PM, Hollingsworth MA, Bromberg J, Costa-Silva B, Peinado H, Kang Y, Garcia BA, O'Reilly EM, Kelsen D, Trippett TM, Jones DR, Matei IR, Jarnagin WR, Lyden D. Extracellular Vesicle and Particle Biomarkers Define Multiple Human Cancers. *Cell*. 2020 Aug 20;182(4):1044-1061.e18. doi: 10.1016/j.cell.2020.07.009.

Hristov M, Erl W, Linder S, Weber PC. Apoptotic bodies from endothelial cells enhance the number and initiate the differentiation of human endothelial progenitor cells in vitro. *Blood*. 2004;104(9):2761-6. doi: 10.1182/blood-2003-10-3614.

Hurst LR, Fratti RA. Lipid Rafts, Sphingolipids, and Ergosterol in Yeast Vacuole Fusion and Maturation. *Front Cell Dev Biol*. 2020 Jul 3;8:539. doi: 10.3389/fcell.2020.00539.

Jeppesen DK, Fenix AM, Franklin JL, Higginbotham JN, Zhang Q, Zimmerman LJ, Liebler DC, Ping J, Liu Q, Evans R, Fissell WH, Patton JG, Rome LH, Burnette DT, Coffey RJ. Reassessment of Exosome Composition. *Cell*. 2019 Apr 4;177(2):428-445.e18. doi: 10.1016/j.cell.2019.02.029.

Jiang L, Paone S, Caruso S, Atkin-Smith GK, Phan TK, Hulett MD, Poon IKH. Determining the contents and cell origins of apoptotic bodies by flow cytometry. *Sci Rep*. 2017 Oct 31;7(1):14444. doi: 10.1038/s41598-017-14305-z.

Jumper J, Evans R, Pritzel A, Green T, Figurnov M, Ronneberger O, Tunyasuvunakool K, Bates R, Židek A, Potapenko A, Bridgland A, Meyer C, Kohl SAA, Ballard AJ, Cowie A, Romera-Paredes B, Nikolov S, Jain R, Adler J, Back T, Petersen S, Reiman D, Clancy E, Zielinski M, Steinegger M, Pacholska M, Berghammer T, Bodenstein S, Silver D, Vinyals O, Senior AW, Kavukcuoglu K, Kohli P, Hassabis D. Highly accurate protein structure prediction with AlphaFold. *Nature*. 2021 Aug;596(7873):583-589. doi: 10.1038/s41586-021-03819-2.

Karkowska-Kuleta J, Kulig K, Karnas E, Zuba-Surma E, Woznicka O, Pyza E, Kuleta P, Osyczka A, Rapala-Kozik M, Kozik A. Characteristics of Extracellular Vesicles Released by the Pathogenic Yeast-Like Fungi *Candida glabrata*, *Candida parapsilosis* and *Candida tropicalis*. *Cells*. 2020 Jul 18;9(7):1722. doi: 10.3390/cells9071722.

Katzmann DJ, Babst M, Emr SD. Ubiquitin-dependent sorting into the multivesicular body pathway requires the function of a conserved endosomal protein sorting complex, ESCRT-I. *Cell*. 2001 Jul 27;106(2):145-55. doi: 10.1016/s0092-8674(01)00434-2..

Katzmann DJ, Odorizzi G, Emr SD. Receptor downregulation and multivesicular-body sorting. *Nat Rev Mol Cell Biol*. 2002 Dec;3(12):893-905. doi: 10.1038/nrm973.

Kogure A, Yoshioka Y, Ochiya T. Extracellular Vesicles in Cancer Metastasis: Potential as Therapeutic Targets and Materials. *Int J Mol Sci*. 2020 Jun 23;21(12):4463. doi: 10.3390/ijms21124463.

Kostelansky MS, Sun J, Lee S, Kim J, Ghirlando R, Hierro A, Emr SD, Hurley JH. Structural and functional organization of the ESCRT-I trafficking complex. *Cell*. 2006 Apr 7;125(1):113-26. doi: 10.1016/j.cell.2006.01.049.

Kostelansky MS, Schluter C, Tam YY, Lee S, Ghirlando R, Beach B, Conibear E, Hurley JH. Molecular architecture and functional model of the complete yeast ESCRT-I heterotetramer. *Cell*. 2007 May 4;129(3):485-98. doi: 10.1016/j.cell.2007.03.016

Kowal J, Tkach M, Théry C. Biogenesis and secretion of exosomes. *Curr Opin Cell Biol*. 2014 Aug;29:116-25. doi: 10.1016/j.ceb.2014.05.004.

Liu J, Cvirkaite-Krupovic V, Commere PH, Yang Y, Zhou F, Forterre P, Shen Y, Krupovic M. Archaeal extracellular vesicles are produced in an ESCRT-dependent manner and promote gene

transfer and nutrient cycling in extreme environments. *ISME J.* 2021 Oct;15(10):2892-2905. doi: 10.1038/s41396-021-00984-0.

Lu Q, Hope LW, Brasch M, Reinhard C, Cohen SN. TSG101 interaction with HRS mediates endosomal trafficking and receptor down-regulation. *Proc Natl Acad Sci U S A.* 2003 Jun 24;100(13):7626-31. doi: 10.1073/pnas.0932599100.

Lv Y, Tan J, Miao Y, Zhang Q. The role of microvesicles and its active molecules in regulating cellular biology. *J Cell Mol Med.* 2019 Dec;23(12):7894-7904. doi: 10.1111/jcmm.14667.

Machtinger R., Laurent L.C., Baccarelli A.A. Extracellular vesicles: Roles in gamete maturation, fertilization and embryo implantation. *Hum. Reprod. Update.* 2016;22:182–193. doi: 10.1093/humupd/dmv055.

Madeira F, Pearce M, Tivey ARN, et al. Search and sequence analysis tools services from EMBL-EBI in 2022. *Nucleic Acids Research.* 2022 Apr;gkac240. doi: 10.1093/nar/gkac240.

Marchesini N, Hannun YA. Acid and neutral sphingomyelinases: roles and mechanisms of regulation. *Biochem Cell Biol.* 2004 Feb;82(1):27-44. doi: 10.1139/o03-091.

Mathivanan S. Extracellular vesicles secreted by *Saccharomyces cerevisiae* are involved in cell wall remodelling. *Commun Biol.* 2019 Aug 9;2:305. doi: 10.1038/s42003-019-0538-8

Menck K, Sivaloganathan S, Bleckmann A, Binder C. Microvesicles in Cancer: Small Size, Large Potential. *Int J Mol Sci.* 2020 Jul 28;21(15):5373. doi: 10.3390/ijms21155373.

Midekessa G, Godakumara K, Ord J, Viil J, Lättekivi F, Dissanayake K, Kopanchuk S, Rinken A, Andronowska A, Bhattacharjee S, Rinken T, Fazeli A. Zeta Potential of Extracellular Vesicles: Toward Understanding the Attributes that Determine Colloidal Stability. *ACS Omega.* 2020 Jun 30;5(27):16701-16710. doi: 10.1021/acsomega.0c01582.

Mobarrez F, Sjövik C, Soop A, Hållström L, Frostell C, Pisetsky DS, Wallén H. CD40L expression in plasma of volunteers following LPS administration: A comparison between assay of CD40L on platelet microvesicles and soluble CD40L. *Platelets.* 2015;26(5):486-90. doi: 10.3109/09537104.2014.932339.

Nishida-Aoki N, Izumi Y, Takeda H, Takahashi M, Ochiya T, Bamba T. Lipidomic Analysis of Cells and Extracellular Vesicles from High- and Low-Metastatic Triple-Negative Breast Cancer. *Metabolites.* 2020 Feb 13;10(2):67. doi: 10.3390/metabo10020067.

Oliveira DL, Nakayasu ES, Joffe LS, Guimarães AJ, Sobreira TJ, Nosanchuk JD, Cordero RJ, Frases S, Casadevall A, Almeida IC, Nimrichter L, Rodrigues ML. Characterization of yeast extracellular vesicles: evidence for the participation of different pathways of cellular traffic in vesicle biogenesis. *PLoS One.* 2010 Jun 14;5(6):e11113. doi: 10.1371/journal.pone.0011113.

Oliver, J. 2021. ‘Saccharomyces cerevisiae communities share extracellular vesicles for protection from heat stress’. MSc (Biology) Thesis. Concordia University. Montreal, QC, Canada.

Platt, F.M., d’Azzo, A., Davidson, B.L. *et al.* Lysosomal storage diseases. *Nat Rev Dis Primers* 4, 27 (2018). <https://doi.org/10.1038/s41572-018-0025-4>

Pornillos O, Alam SL, Davis DR, Sundquist WI. Structure of the Tsg101 UEV domain in complex with the PTAP motif of the HIV-1 p6 protein. *Nat Struct Biol.* 2002 Nov;9(11):812-7. doi: 10.1038/nsb856.

Pornillos O, Alam SL, Rich RL, Myszka DG, Davis DR, Sundquist WI. Structure and functional interactions of the Tsg101 UEV domain. *EMBO J.* 2002 May 15;21(10):2397-406. doi: 10.1093/emboj/21.10.2397.

Poupardin R, Wolf M, Strunk D. Adherence to minimal experimental requirements for defining extracellular vesicles and their functions. *Adv Drug Deliv Rev.* 2021 Sep;176:113872. doi: 10.1016/j.addr.2021.113872.

Regimbeau M, Abrey J, Vautrot V, Causse S, Gobbo J, Garrido C. Heat shock proteins and exosomes in cancer theranostics. *Semin Cancer Biol.* 2022 Nov;86(Pt 1):46-57. doi: 10.1016/j.semcancer.2021.07.014..

Rizzo, J., Taheraly, Adam., Janbon, G. 2021. *Structure, composition and biological properties of fungal extracellular vesicles. microLife*, Volume 2, 2021, uqab009. doi.org/10.1093/femsml/uqab009

Rodrigues TA, Tuna KM, Alli AA, Tribulo P, Hansen PJ, Koh J, Paula-Lopes FF. Follicular fluid exosomes act on the bovine oocyte to improve oocyte competence to support development and survival to heat shock. *Reprod Fertil Dev.* 2019 Apr;31(5):888-897. doi: 10.1071/RD18450.

Safary A, Akbarzadeh Khiavi M, Mousavi R, Barar J, Rafi MA. Enzyme replacement therapies: what is the best option? *Bioimpacts.* 2018;8(3):153-157. doi: 10.15171/bi.2018.17.

Saksena S, Sun J, Chu T, Emr SD. ESCRTing proteins in the endocytic pathway. *Trends Biochem Sci.* 2007 Dec;32(12):561-73. doi: 10.1016/j.tibs.2007.09.010.

Santavanond JP, Rutter SF, Atkin-Smith GK, Poon IKH. Apoptotic Bodies: Mechanism of Formation, Isolation and Functional Relevance. *Subcell Biochem.* 2021;97:61-88. doi: 10.1007/978-3-030-67171-6_4.

Schmidt O, Teis D. The ESCRT machinery. *Current Biology : CB.* 2012 Feb;22(4):R116-20. doi: 10.1016/j.cub.2012.01.028.

Shao C, Yang F, Miao S, Liu W, Wang C, Shu Y, Shen H. Role of hypoxia-induced exosomes in tumor biology. *Mol Cancer.* 2018 Aug 11;17(1):120. doi: 10.1186/s12943-018-0869-y.

Skaar K, Korza HJ, Tarry M, Sekyrova P, Högbom M. Expression and Subcellular Distribution of GFP-Tagged Human Tetraspanin Proteins in *Saccharomyces cerevisiae*. *PLoS One*. 2015 Jul 28;10(7):e0134041. doi: 10.1371/journal.pone.0134041.

Skryabin GO, Komelkov AV, Savelyeva EE, Tchekina EM. Lipid Rafts in Exosome Biogenesis. *Biochemistry (Mosc)*. 2020 Feb;85(2):177-191. doi: 10.1134/S0006297920020054.

Slagsvold T, Pattni K, Malerød L, Stenmark H. Endosomal and non-endosomal functions of ESCRT proteins. *Trends Cell Biol*. 2006 Jun;16(6):317-26. doi: 10.1016/j.tcb.2006.04.004.

Sundquist WI, Schubert HL, Kelly BN, Hill GC, Holton JM, Hill CP. Ubiquitin recognition by the human TSG101 protein. *Mol Cell*. 2004 Mar 26;13(6):783-9. doi: 10.1016/s1097-2765(04)00129-7.

Taniguchi M, Okazaki T. Role of ceramide/sphingomyelin (SM) balance regulated through "SM cycle" in cancer. *Cell Signal*. 2021 Nov;87:110119. doi: 10.1016/j.cellsig.2021.110119.

The UniProt Consortium 2021. UniProt: the universal protein knowledge database in 2021. *Nucleic Acids Res*. 49:D480-D489(2021).

They, C., M. Boussac, P. Veron, P. Ricciardi-Castagnoli, G. Raposo, J. Garin, and S. Amigorena. 2001. Proteomic analysis of dendritic cell-derived exosomes: a secreted subcellular compartment distinct from apoptotic vesicles. *J Immunol*. 166:7309-7318. doi:10.4049/jimmunol.166.12.7309.

They, C., M. Ostrowski, and E. Segura. 2009. Membrane vesicles as conveyors of immune responses. *Nature reviews*. 9:581-593. doi: 10.1038/nri2567

They, C., Witwer KW, Aikawa E., et al. 2018. Minimal information for studies of extracellular vesicles 2018 (MISEV2018): a position statement of the International Society for Extracellular Vesicles and update of the MISEV2014 guidelines. *J Extracell Vesicles*. 2018 Nov 23;7(1):1535750. doi: 10.1080/20013078.2018.1535750.

Tucher C, Bode K, Schiller P, Claßen L, Birr C, Souto-Carneiro MM, Blank N, Lorenz HM, Schiller M. Extracellular Vesicle Subtypes Released From Activated or Apoptotic T-Lymphocytes Carry a Specific and Stimulus-Dependent Protein Cargo. *Front Immunol*. 2018 Mar 15;9:534. doi: 10.3389/fimmu.2018.00534..

Varadi, M., et al. 2021. Alpha Fold Protein Structure Database: massively expanding the structural coverage of protein-sequence space with high-accuracy models. *Nucleic Acids Research*.

Villarroya-Beltri C, Baixauli F, Gutiérrez-Vázquez C, Sánchez-Madrid F, Mittelbrunn M. Sorting it out: regulation of exosome loading. *Semin Cancer Biol.* 2014 Oct;28:3-13. doi: 10.1016/j.semcancer.2014.04.009.

Wijenayake S, Eisha S, Tawhidi Z, Pitino MA, Steele MA, Fleming AS, McGowan PO. Comparison of methods for pre-processing, exosome isolation, and RNA extraction in unpasteurized bovine and human milk. *PLoS One.* 2021 Sep 30;16(9):e0257633. doi: 10.1371/journal.pone.0257633.

Willms E, Cabañas C, Mäger I, Wood MJA, Vader P. Extracellular Vesicle Heterogeneity: Subpopulations, Isolation Techniques, and Diverse Functions in Cancer Progression. *Front Immunol.* 2018 Apr 30;9:738. doi: 10.3389/fimmu.2018.00738

Yáñez-Mó M, Siljander PR, Andreu Z, Zavec AB, Borràs FE, Buzas EI, Buzas K, Casal E, Cappello F, Carvalho J, Colás E, Cordeiro-da Silva A, Fais S, Falcon-Perez JM, Ghobrial IM, Giebel B, Gimona M, Graner M, Gursel I, Gursel M, Heegaard NH, Hendrix A, Kierulf P, Kokubun K, Kosanovic M, Kralj-Iglic V, Krämer-Albers EM, Laitinen S, Lässer C, Lener T, Ligeti E, Linē A, Lipps G, Llorente A, Lötvalld J, Manček-Keber M, Marcilla A, Mittelbrunn M, Nazarenko I, Nolte-t Hoen EN, Nyman TA, O'Driscoll L, Oliván M, Oliveira C, Pállinger É, Del Portillo HA, Reventós J, Rigau M, Rohde E, Sammar M, Sánchez-Madrid F, Santarém N, Schallmoser K, Ostfeld MS, Stoorvogel W, Stukelj R, Van der Grein SG, Vasconcelos MH, Wauben MH, De Wever O. Biological properties of extracellular vesicles and their physiological functions. *J Extracell Vesicles.* 2015 May 14;4:27066. doi: 10.3402/jev.v4.27066.

Yang Y, Wang Y, Wei S, Zhou C, Yu J, Wang G, Wang W, Zhao L. Extracellular vesicles isolated by size-exclusion chromatography present suitability for RNomics analysis in plasma. *J Transl Med.* 2021 Mar 12;19(1):104. doi: 10.1186/s12967-021-02775-9.

Yu S, Cao H, Shen B, Feng J. Tumor-derived exosomes in cancer progression and treatment failure. *Oncotarget.* 2015 Nov 10;6(35):37151-68. doi: 10.18632/oncotarget.6022.

Zaborowski MP, Balaj L, Breakefield XO, Lai CP. Extracellular Vesicles: Composition, Biological Relevance, and Methods of Study. *Bioscience.* 2015 Aug 1;65(8):783-797. doi: 10.1093/biosci/biv084.

Zamith-Miranda D, Peres da Silva R, Couvillion SP, Bredeweg EL, Burnet MC, Coelho C, Camacho E, Nimrichter L, Puccia R, Almeida IC, Casadevall A, Rodrigues ML, Alves LR, Nosanchuk JD, Nakayasu ES. Omics Approaches for Understanding Biogenesis, Composition and Functions of Fungal Extracellular Vesicles. *Front Genet.* 2021 May 3;12:648524. doi: 10.3389/fgene.2021.648524

Zhang Y, Liu Y, Liu H, Tang WH. 2019. Exosomes: biogenesis, biologic function and clinical potential. *Cell Biosci.* 2019 Feb 15;9:19. doi: 10.1186/s13578-019-0282-2.

Zhao K, Bleackley M, Chisanga D, Gangoda L, Fonseka P, Liem M, Kalra H, Al Saffar H, Keerthikumar S, Ang CS, Adda CG, Jiang L, Yap K, Poon IK, Lock P, Bulone V, Anderson M,

Mathivanan S. Extracellular vesicles secreted by *Saccharomyces cerevisiae* are involved in cell wall remodelling. *Commun Biol.* 2019 Aug 9;2:305. doi: 10.1038/s42003-019-0538-8.

Zhu S, Li S, Yi M, Li N, Wu K. Roles of Microvesicles in Tumor Progression and Clinical Applications. *Int J Nanomedicine.* 2021 Oct 18;16:7071-7090. doi: 10.2147/IJN.S325448.